Post-collision interaction in atomic processes

M. Yu. Kuchiev and S. A. Sheĭnerman

A. F. Ioffe Physicotechnical Institute, Academy of Sciences of the USSR, Leningrad
Usp. Fiz. Nauk **158**, 353–387 (July 1989)

The review examines the interaction of several charged particles in the final state of processes in the case when the reaction proceeds in two stages through an intermediate resonance. In an inelastic collision of arbitrary atomic particles X and Y a particle D is formed in a quasistationary state along with particle A: $X + Y \to A + D$. As a result of the breakup $D \to B + C$ charged particles A, B, and C are formed in the final state. The Coulomb interaction of these particles (the post-collision interaction—PCI) exerts a strong influence on the cross section for the process. Reactions in which the effects of PCI are manifested are the excitation of atomic autoionized states by ions and electrons and the ionization of inner shells of atoms by collisions with ions, electrons or photons followed by Auger decay. Under the influence of PCI the spectra of the products of these reactions are distorted: the lines in the autoionization spectrum are broadened, shifted, and become asymmetric. A survey is given of the available theoretical concepts concerning PCI and of the accumulated experimental data providing evidence of its manifestation. The kinematic region in which the problem has a parametrically exact analytic solution is investigated thoroughly. Post-collision interaction in more complex processes in the final state of which four charged particles are involved is also examined. Experiments are discussed that make it possible to observe new manifestations of PCI. Various interference effects in PCI are examined.

1. INTRODUCTION

This paper is devoted to a review of a specific range of phenomena in atomic physics, which is referred to throughout the literature as the *post-collision interaction* (PCI). The physical interpretation of this somewhat strange designation is as follows. Consider a process involving the inelastic collision between two arbitrary atomic particles X and Y that results in the appearance of two other atomic particles A and D. Particle D is in an excited quasistationary state and decays with the formation of particles B and C. The overall scheme for this process can be written in the form

$$X + Y \to A + D \to A + B + C. \qquad (1.1)$$

We shall suppose that all three particles A, B, and C are charged in the final state of reaction (1.1). Their Coulomb interaction is referred to as post-collisional. In other words, it is the interaction between a number of charged particles in the final state, when the reaction occurs in two stages via an intermediate resonance.

It is clear that if the relative velocities of particles A, B, and C in reaction (1.1) are low, and in fact lower than the Bohr velocity, their Coulomb interaction must be regarded as significant. It has a strong effect on the cross section for the process and modifies the energy and angular distributions of the particles. It is therefore essential to take it into account. However, this requires the quantum-mechanical solution of the problem of three charged particles, which is relatively difficult.

One of our aims in this review is methodological. We wish to show that the problem of post-collision interaction in reaction (1.1) is actually quite simple and has a parametrically exact analytic solution. Once we have this in hand, we can predict the energy and angular distributions of particles A, B, and C. These distributions undergo a very significant change as the post-collisional kinematics is varied. This leads us to the second aim of our review, namely, to draw the attention of experimenters to a number of new observable effects.

Finally, our third aim is to systematize the extensive theoretical ideas now available on the nature of the phenomenon, and to provide a brief review of existing experimental data. A review of early work in this area can be found in Refs. 1 and 2. Closely associated questions are discussed in the review by Matveev and Parilis.[3]

We shall now discuss the phenomena due to the post-collision interaction. With this in view, we shall be interested in the energy spectrum of the pair B, C for a given collision energy in (1.1). At first, we shall assume that the Coulomb interaction between the particles does not play an appreciable part (this can happen, for example, when the velocity of particle A is high). The spectrum of B and C then contains the Lorentz line due to the quasistationarity of the parent particle D. In other words, the combined energy of the pair B, C is almost exactly equal to the energy of particle D, and the linewidth is then the total width of the quasistationary state.

The characteristic feature of the post-collision interaction is that this line is highly distorted: it is shifted, i.e., the pair B, C exchanges energy with the third particle A, and has its own particular shape, i.e., it broadens and becomes asymmetric.

These phenomena were first observed by Barker and Berry[4] who examined the excitation of autoionizing states of atoms in collisions with slow ions, i.e.,

$$I + A \to I + A^* \to I + A^* + e. \qquad (1.2)$$

The target was the helium atom and the projectile was He^+ or Ne^+ ion. The spectrum of autoionization electrons was observed and it was found that the spectral line corresponding to the decay of the $(2s2p)$ state of He^+ was shifted toward lower energies and became broadened as the collision energy was reduced from 4 to 1 KeV.

 0038-5670/89/070569-19$01.80

A simple physical model was proposed[4] to explain the observed phenomenon. The model was based on the assumption that, as it moves along its classical trajectory, the slow scattered ion experiences the sudden change in the field of the target atom that is due to the decay of the quasistationary state of the atom. The scattered ion is accelerated in this process by the Coulomb field of the target ion, and its energy increases. The departing autoionization electron is slowed down by the Coulomb field of the projectile ion, i.e., there is an energy transfer between the emitted particles that is exactly equal to the change in the potential energy of the scattered ion in the field of the target $1/R(t)$ where $R(t)$ is the distance between the atom and the scattered ion at the time of decay. The decay probability at time t is given by the exponential law $P \sim \exp(-t/\tau)$ where τ is the lifetime of the autoionizing state ($\tau = \hbar\Gamma^{-1}$) and Γ is its width. This decay law leads to the following expression for the probability density describing the exchange of energy ε as the particles leave the reaction region:

$$P(\varepsilon) = \exp\left(-\frac{\Gamma}{\varepsilon V}\right)\Gamma(\varepsilon^2 V)^{-1}. \tag{1.3}$$

The distribution $P(\varepsilon)$ is determined by the width Γ and the velocity V of the scattered ion. The maximum of the distribution (1.3) corresponds to the following most probable transfer of energy:

$$\Delta\varepsilon = \frac{\Gamma}{2V}. \tag{1.4}$$

This expression explains the reduction in the energy of the autoionization electron with decreasing velocity V of the scattered ion.

The proposed classical model of the post-collision interaction rests not only on the assumption of a sudden change in the field of the target atom, but also on the assumption that the mean lifetime τ is unaffected by the presence of the scattered ion. The role of the interaction is then reduced to the transfer of energy between particles leaving the reaction region. This model provides at least a qualitative explanation of the observed phenomenon. During the 20 years following the first observation of the post-collision effects, the phenomenon has been extensively studied not only in processes such as (1.2), but also in other reactions. First, these effects were extensively studied in processes involving the excitation of autoionizing states of atoms by electron impact[1,5-8]

$$e + A \to e_1 + A^* \to e_1 + e_2 + A^+, \tag{1.5}$$

and also in the photoionization of the inner shells of atoms, followed by Auger decay[2]

$$h\nu + A \to e_1 + A^{+*} \to e_1 + e_2 + A^{2+}. \tag{1.6}$$

Experimental evidence was obtained for the post-collision interaction during the excitation of autoionizing states[5,6,8-13] and the ionization of inner shells[14-16] of several atoms (mostly inert gases). Different theoretical approaches[8,17-24] were developed to explain the observed phenomena.

The interaction between particles in the final state of resonance processes is also significant in reactions that are more complicated than (1.1). In particular, it can be seen in reactions with four charged particles in the final state. These states arise during the ionization of the inner shells of ions by ion or electron impact, followed by the Auger decay of the resulting vacancy:

$$I + A \to I + e_1 + A^{+*} \to I + e_1 + e_2 + A^{2+}, \tag{1.7}$$

$$e + A \to e_1 + e_2 + A^{+*} \to e_1 + e_2 + e_3 + A^{2+}. \tag{1.8}$$

These processes have been under extensive experimental investigation[25-30] and, in recent years, theoretical investigation as well.[24,31-33] Of course, these reactions are more difficult to describe theoretically and to investigate experimentally than reaction (1.1).

A final state containing particles A, B, and C can also be due to a direct nonresonance inelastic collision that is coherent with (1.1), i.e.,

$$X + Y \to A + B + C. \tag{1.9}$$

The interaction between particles in the final state of this process is also significant in the theoretical description,[34,35] and is also sometimes referred to as the post-collision interaction.[36] However, it seems more natural to confine the phrase *post-collision interaction* to resonance phenomena such as (1.1).

When experimental data on the spectrum of particles A, B, and C are interpreted, it is frequently difficult to separate the direct process (1.9) from the resonance processes (1.1). The observed particle distribution is then determined by the sum of the amplitudes for processes (1.1) and (1.9), and the role of the post-collision interaction is significant and leads to oscillations in the spectrum that are different from the characteristic Fano contour.[37] Interesting effects are observed not only during interference between direct and resonance amplitudes, but also during the interference of resonance processes proceeding via the formation of different intermediate quasistationary states.[19,38] A complicated oscillatory structure, whose form is determined by the parameters of the autoionizing state and the kinematics of the emitted particles, is produced in this process.

Despite the diversity of processes in which PCI can be seen, its salient features can be investigated by considering reaction (1.1), and significant advances were recently achieved in the theoretical description of this reaction.[23,24,39] The results of these analyses are presented in Section 2, where it is shown that the complicated quantum-mechanical three-body problem can be substantially simplified for these processes. First, it can be reduced to the quasiclassical problem and, second, it only needs to be solved for large separations between the emitted particles. The importance of large distances is emphasized by the fact that the widths of the quasistationary atomic states are usually small. Moreover, since the distances are large, we can disregard the internal structure of the particles and confine our attention to the Coulomb interaction alone.

Thus, the post-collision interaction reduces to the problem of three charged bodies moving at large distances from one another. The problem has a parametrically exact solution, given by the eikonal approximation. The final solution can be written in simple analytic form that is valid in a wide range of energies and emission angles of the particles produced in the reaction.

We emphasize that this approach is based on the problem of three bodies at large distances from one another. The

problem has often been encountered before and is well known. We recall two situations in which it has played an important part.

The first is the exchange interaction between atoms at large distances.[116–118] The problem is examined in Refs. 116 and 117 for atomic hydrogen, and more complicated atoms are discussed in Ref. 118. The salient feature is the behavior of the wave functions of the two electrons well away from the two ions, and the field of the ions plays the role of the third body.

The second problem is the behavior of the exchange amplitude for the elastic scattering of an electron by an atom in the case of negative (nonphysical) energy.[119] It is found that the amplitude has an unusual singularity at which the energy of the electron is equal to the binding energy of the atom. The singularity is due to the behavior of the wave function at large distances between the incident electron, the ion, and the electron leaving the atom.

It is interesting that problems that are fundamentally different in their formulation have a common basis, namely, the problem of three charged particles that interact at large distances between them. In the two examples mentioned above, the motion takes place under the barrier and with negative energies. In contrast, the problem of post-collision interaction rests on the fact that the motion of the particles occurs in the continuum, i.e., in the classically allowed region.

The plan of our presentation is as follows. In Section 3, we consider the traditionally studied region of manifestations of post-collision interaction, i.e., the region of near-threshold excitation. In Section 4, we examine three-particle effects in the final state of reaction (1.1). In Section 5, we consider PCI in reactions with four charged particles in the final state. Next, we investigate the role of PCI in interference effects and, in the concluding Section, we discuss certain other aspects of our problem, e.g., the exchange of angular momentum.

2. EXACT SOLUTION OF THE PROBLEM OF REACTIONS WITH THREE PARTICLES IN THE FINAL STATE

Consider (1.1) with three charged particles in the final state of the reaction. It is found that, when PCI is taken into account, the problem has a parametrically exact solution in a wide range of velocities and angles of emission of the resulting particles.[23,40] Remarkably, the solution has a simple analytic form.

First, we note that the PCI problem in atomic collision processes involves a small parameter, namely, the width Γ of the autoionizing state. Usually, $\Gamma < 1$ eV $\ll 1$ atomic units (here and henceforth we use atomic units defined by $|e| = \hbar = m_e = 1$). Accordingly, the atomic excited-state lifetime is very long, i.e., $\tau = 1/\Gamma \gg 1$. We shall suppose that the relative velocity V_{AD} of particles A and D is not too small, so that the distance between them at the time of decay of the quasistationary state of D is large. If we adopt these assumptions, this distance is

$$r_{AD} \approx \frac{V_{AD}}{\Gamma} \equiv R \gg 1. \tag{2.1}$$

Here and henceforth we use the following notation: $r_{ij} = |\mathbf{r}_i - \mathbf{r}_j|$, $V_{ij} = \mathbf{V}_i - \mathbf{V}_j|$, and $\mathbf{r}_i$, $\mathbf{V}_i$ are the position vector and velocity of particle i, respectively.

We note that the Coulomb interaction between particles A and D does not affect the estimate given by (2.1), which implies that particle A has no effect on the decay of particle D. Moreover, we conclude that the interaction between A, on the one hand, and B and C produced in the reaction, on the other, is largely due to Coulomb forces. The internal structure of the particles, their polarizability, van der Waals attraction, etc., play a very much smaller part and will be ignored.

Let us determine what happens as B and C separate. So long as the separation r_{BC} between the particles is small ($r_{BC} \ll R$), the Coulomb interaction between A and the B, C pair is not very different from the interaction between A and the parent particle D alone. Consequently, this is the ordinary two-body Coulomb problem. The interaction between B and C at short distances can be strong and complicated, and necessarily involves the structure of these particles. The important point is that the weak field of the distant particle A has no effect on the relative motion of the pair B-C.

The situation changes when distance r_{BC} becomes large, i.e., $r_{BC} \gtrsim R$. Here we do actually encounter the three-body problem in which we must take into account the Coulomb interaction between all three particles A, B, and C. However, there is one simplifying feature. Since the separations between all the particles are large, i.e.,

$$r_{AB} \approx r_{AC} \approx r_{BC} \approx R \gg 1, \tag{2.2}$$

we may suppose that the potential energy of the interaction is small. We shall, in fact, assume that it is less than the kinetic energy of each pair:

$$\frac{|z_A z_B|}{r_{AB}} \ll \varepsilon_{AB}, \quad \frac{|z_A z_C|}{r_{AC}} \ll \varepsilon_{AC}, \quad \frac{|z_B z_C|}{r_{BC}} \ll \varepsilon_{BC}; \tag{2.3}$$

where Z_i is the charge of particle i and $\varepsilon_{ij} = m_i m_j (m_i + m_j)^{-1} V_{ij}^2/2$ is the relative kinetic energy of the pair ij in the center of mass system. The inequalities given by (2.3) guarantee that the quantum-mechanical Coulomb problem of three bodies reduces to the quasiclassical problem in region (2.2). Moreover, the particle trajectories are almost rectilinear and uniform. In other words, the quasiclassical problem reduces to its simplest eikonal form.

We shall not reproduce a rigorous derivation of the expression for the amplitude for process (1.1) with allowance for PCI. This derivation is relatively laborious,[23,40] but the final answer is simple and can be obtained by qualitative considerations. The amplitude is given by

$$M_{X,Y\to A,B,C} = M_1 M_2 (-i) \int_0^\infty dt \exp\left\{ i \left[\left(\varepsilon + i \frac{\Gamma}{2} \right) t - \int_0^T d\tau U(t, \tau) \right] \right\} \tag{2.4}$$

where M_1 is the amplitude for the inelastic scattering of particles X, Y with the formation of particles A and D, and M_2 is the amplitude (matrix element) for the decay of particle D. These amplitudes occur naturally in (2.4). The point is that large distances (2.1) are then significant, and the corresponding wave function that describes the separating particles A and D is characterized by the amplitude M_1. In pre-

cisely the same way, the wave function of the pair B, C is characterized by the amplitude M_2 at large distances. We note that the strong interaction within the pairs, A, D and B, C at short distances R_{AD} and R_{BC} is accurately taken into account in the amplitudes M_1 and M_2. The integration variable t in (2.4) can be interpreted as the time that has elapsed between collision and decay. The energy variable ε in (2.4) is given by

$$\varepsilon = E_A + E_D - E_X - E_Y, \tag{2.5}$$

where E_i is the sum of the internal and kinetic energies of the ith particle.

The variable τ in (2.4) is the time that has elapsed since the decay of D and $U(t,\tau)$ is the change in the potential energy of the system due to the decay:

$$U(t,\tau) = z_A z_B |\mathbf{V}_{AD} t + \mathbf{V}_{AB}\tau|^{-1} + z_A z_C |\mathbf{V}_{AD} t + \mathbf{V}_{AC}\tau|^{-1} - z_A z_D V_{AD}^{-1} (t+\tau)^{-1}. \tag{2.6}$$

The negative sign in front of the third term is due to the "disappearance" of particle D as a result of decay.

The term $\int U(t,\tau)d\tau$ in (2.4) has a simple physical interpretation: it is the classical action calculated for rectilinear trajectories. It is indeed this term that is responsible for the interaction in the final state, i.e., for PCI. When it is neglected, (2.4) describes the usual Breit-Wigner resonance amplitude.

If we use (2.6) for the potential, we can readily find the explicit analytic form of the amplitude (2.4). To obtain the cross section for the process, it is sufficient to determine the square of the modulus of the resulting amplitude. We note that the cross section does not depend on the upper limit of the integral with respect to τ. To be specific, we shall confine our attention to the collision process (1.1) with fixed incident-particle velocities $\mathbf{V}_A, \mathbf{V}_B, \mathbf{V}_C$. Because of the conservation of energy and of momentum, the cross section is then determined by five independent parameters, e.g., the energy, the direction of emission of one of the particles E_A, Ω_A, and the direction of emission of another particle Ω_B. Simple analysis then yields the following expression for the cross section:

$$\frac{d^5\sigma}{dE_A d\Omega_A d\Omega_B} = \sigma_0 \frac{\Gamma_{BC}}{2\pi[\varepsilon^2 + (\Gamma^2/4)]} k(\xi, \varepsilon), \tag{2.7}$$

$$k(\xi, \varepsilon) = \frac{\pi\xi}{\mathrm{sh}(\pi\xi)} \exp\left(2\xi \operatorname{arctg} \frac{2\varepsilon}{\Gamma}\right); \tag{2.8}$$

where Γ_{BC} represents the partial width for the decay $D \to B + C$ that is determined by the amplitude M_2. The cross section σ_0 for the process $X + Y \to A + D$ is determined by the amplitude M_1. The dimensionless parameter ξ is the basic parameter of the theory. It depends only on the kinematics of the particle leaving the event:

$$\xi = \xi_{AB} + \xi_{AC} - \xi_{AD} = \frac{z_A z_B}{V_{AB}} + \frac{z_A z_C}{V_{AC}} - \frac{z_A z_D}{V_{AD}}. \tag{2.9}$$

The cross section given by (2.7) describes all the salient features of PCI. The first two factors in this cross section describe the usual Breit-Wigner resonance. The factor $k(\xi,\varepsilon)$ represents the interaction between the particles in the final state. It depends on ε via the ratio ε/Γ and, consequently, varies rapidly across the line width, which leads to a strong distortion of the Lorentz profile. Simple analysis of (2.7) then shows that it describes the following distortions in the spectrum:

1. The line maximum is shifted by the amount $\Delta\varepsilon$, given by

$$\Delta\varepsilon = \frac{\xi\Gamma}{2}. \tag{2.10}$$

2. The line intensity at the maximum decreases monotonically with increasing $|\xi|$:

$$\left(\frac{d^5\sigma}{dE_A d\Omega_A d\Omega_B}\right)_{\max} = \frac{2\sigma_0\Gamma_{BC}}{\Gamma^2} \frac{\xi}{(1+\xi^2)\,\mathrm{sh}(\pi\xi)} \exp(2\xi \operatorname{arctg} \xi). \tag{2.11}$$

For large $|\xi|, |\xi| \gg 1$, the function (2.11) decreases as $|\xi|^{-1}$ This is accompanied by a broadening of the line that occurs so that the total line intensity remains constant. The line width at half height, $\tilde{\Gamma}$, is proportional to $|\xi|$ for large $|\xi|$:

$$\tilde{\Gamma} = \text{const} \cdot |\xi|. \tag{2.12}$$

3. The line becomes asymmetric. It declines more slowly as ε increases, and the asymmetry becomes more pronounced as $|\xi|$ increases.

All the changes in the spectrum depend on the single parameter ξ. The distortion of the spectrum is greater for greater $|\xi|$. Moreover, all the manifestations of PCI depend on the sign of ξ. The important point here is that the conditions for the validity of the above theory, given by (2.1)–(2.3), do not exclude situations for which the velocities V_{AD}, V_{AB}, V_{AC} (all or some of them) are less than unity. It follows that $|\xi|$ can be greater than unity and, consequently, the changes in the spectrum can be quite considerable.

We must now show how the general formulas become modified when applied to particular processes such as (1.2), (1.5), and (1.6) in which A is a scattered ion or electron [photoelectron for (1.6) or scattered electron for (1.5)], B is an autoionization or Auger electron, and D and C are atomic particles that we assume to be heavy. Hence $\mathbf{V}_D \approx \mathbf{V}_C \approx 0$. We then find that (2.9) becomes

$$\xi = -z_A z_B (V_A^{-1} - V_{AB}^{-1}). \tag{2.13}$$

Formulas (2.7), (2.8), and (2.13) describe the effect of PCI on the angular and energy distributions of the products of reactions (1.2), (1.5), and (1.6). The parameter ξ is very dependent on the velocities and angles of emission of particles A and B departing from the ion. Hence the PCI effects are also very dependent on the kinematics of these reactions. These features will be discussed in greater detail in Section 4.

We now note the following point. The cross sections for processes (1.5) and (1.6) are given by (2.7) if both emitted electrons are recorded in the final state. However, the simplest and the most common experimental method of investigating PCI is to study the spectrum of only one particle, e.g., the autoionization or Auger electron. This spectrum is described by the cross section (2.7) integrated with respect to the emission angle of particle A. Both the function $k(\xi,\varepsilon)$ and the cross section σ_0 depend on this angle. This means

that, in general, the cross section $d^3\sigma/dE_B d\Omega_B$ cannot be written in an analytic form. However, the shift of the autoionization line measured in such experiments can be estimated for two simple models.[23] In the lowest order approximation, the line shift in the spectrum of particle B is measured simply by the shift (2.10) averaged over the angle of emission of particle A:

$$\overline{\Delta\varepsilon} = \frac{1}{4\pi}\int \Delta\varepsilon \, d\Omega_A = -\frac{\Gamma z_A z_B}{2V_A} \times \begin{cases} 1 - \dfrac{V_A}{V_B}, & V_B \geqslant V_A, \\ 0, & V_B \leqslant V_A, \end{cases} \tag{2.14}$$

where $\Delta\varepsilon$ is given by (2.10). A more accurate estimate for the line shift $\Delta\varepsilon(\bar{\sigma})$ can be obtained by taking an average of the cross section (2.7) over the angles of emission of particle A, assuming that the cross section σ_0 is isotropic. It is indeed the shift of the average cross section $\Delta\varepsilon(\bar{\sigma})$ that is measured in the experiments mentioned above.

The eikonal formula (2.7) gives the parametrically exact solution of the problem. Several model approaches, each of which reproduces to some extent the results of the eikonal theory, are given in the literature. They are briefly discussed below.

First, we recall Ref. 41 which served as a stimulus to the investigation of three-body effects in PCI. It was based on a qualitative analysis of the classical picture of particles leaving the event, and proposed (2.14) for the line shift due to the post-collision interaction. The expression was confirmed in Ref. 42 by a direct numerical solution of the classical three-body Coulomb problem.

The approximate expression for the energy shift of the autoionization electron was obtained in Ref. 43 by analyzing the classical picture of the separation of particles in ion-atom collisions. For $V_A \gg V_B$ this reduces to the eikonal case. For $V_A \lesssim V_B$ the relations obtained are found to be unsuitable. A more detailed discussion of this problem is given in Refs. 39 and 44 where the classical approach is used to derive (2.10) and (2.13) for the energy shift of the autoionization electron. Expression (2.7) for the line profile in the spectrum of autoionization electrons was also obtained in Ref. 44. The classical approach, used to derive the expression for the energy shift, was combined with the quantum-mechanical approach, developed earlier in Ref. 45 for the description of the autoionization electron line profile.

Three-body PCI effects were described in Refs. 24 and 26 by models developed earlier in Ref. 47 and 48 for the near-threshold region (see Section 3). The three-body character of the problem was accounted for in the model by introducing a velocity-dependent effective charge of the resulting ion. Despite the differences of approach used to derive the above formulas, the results based on the models given in Refs. 24 and 46 were found to be equivalent. They satisfactorily reproduce the formulas of the eikonal theory for $V_B \geqslant V_A$, provided these formulas were averaged over the angles of emission of particle A.

Finally, we recall Ref. 114 in which the problem was solved by using the three-particle theory of scattering of charged particles. The amplitude for process (1.1) was obtained in the diagonalization approximation, and was found to reduce to (2.4) in the range in which the eikonal approximation was valid.

3. REGION OF NEAR-THRESHOLD EXCITATIONS

Expressions (2.9) and (2.10) show that the PCI effect increases with decreasing relative velocity of any pair of particles leaving the reaction. It is therefore not surprising that processes with this type of kinematics have been examined in considerable detail. We shall discuss them in this Section. They are observed, for example, when the scattered particle in reactions (1.2) and (1.5), or the photoelectron in process (1.6), have a low velocity $V_A \ll 1$. For reactions (1.5) and (1.6), this situation occurs when the energy of the scattered electron or photoelectron amounts to a few electron volts.

Usually, the velocity of the Auger or autoionization electron is high: $V_B \gtrsim 1$. This ensures that the inequality $V_B \gg V_A$ is satisfied in this case, and the parameter ξ given by (2.13) assumes the form

$$\xi = -\frac{z_A z_B}{V_A}. \tag{3.1}$$

The shift (2.10) is then identical with the Barker-Berry formula.[4] An important conclusion may be drawn from (3.1): PCI effects in the near-threshold region do not depend on the direction of emission of the autoionization electron.

Before we examine the PCI theory in the near-threshold region in greater detail, let us pause to consider the extensive experimental data that are now available. As noted in the Introduction, experimental studies of PCI effects in the near-threshold region began with the paper by Barker and Berry,[4] who studied the autoionization spectrum of electrons emitted in collisions between slow ions He^+ and Ne^+ and helium atoms. The essential role of PCI in these processes manifested itself in the shift of the autoionization electron peaks (the energy of the autoionization electrons was reduced by PCI) and in the line broadening observed as the incident-ion energy was varied. The same effects were observed in the spectra of autoionizing electrons produced in ion-atom collisions such as $He^+ + He$, $Ne^+ + Ne$, $Ar^+ + Ar$, and $Kr^+ + Kr$ (Ref. 49). PCI was also intensively investigated in processes involving the excitation of autoionizing states of ions by electron impact.[5,6,8,13,50,51] The lowest autoionizing states of the helium atom, and also those of magnesium[51] and argon,[13] were most frequently investigated. The energy transfer occuring in these processes as a result of PCI ensured that the slow scattered electron was retarded even more, whereas the fast autoionization electron was accelerated. The effect observed in the autoionization spectra of electrons, which was due to the shift of the individual lines, was opposite in sign to the effect observed for (1.2) (see Fig. 1). The opposite sign was due to the negative charge of the scattered particle. The line shift effect was also observed in the spectrum of scattered electrons when the autoionization spectrum of helium and neon was excited by electron impact.[9,52]

As the incident-electron energy is reduced, the energy transfer due to PCI may become comparable in magnitude with the energy excess of the incident electron above the excitation threshold. This ensures that the scattered electron loses energy, either partially or completely, as a result of PCI. Detection of zero-energy scattered electrons then corresponds to the observation of a shift of the threshold energy for AIS.[1,6]

If the energy excess E_1 of the scattered electron above

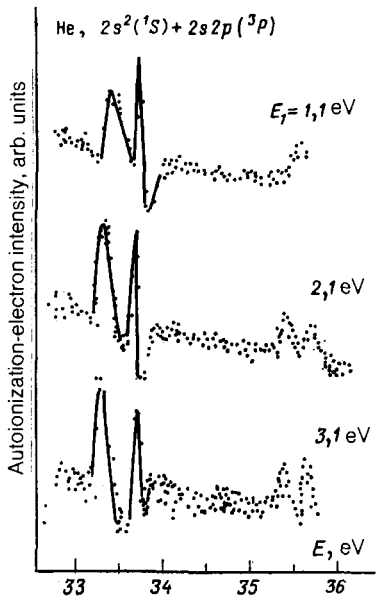

FIG. 1. Spectrum of autoionization electrons recorded during the excitation of the $2s^2(^1S)$ and $2s2p^3P$ states of helium by electron impact.[5] Angle of observation 70°, E_1-energy excess of incident electrons above the excitation threshold.

the AIS excitation threshold is small enough, the energy $\Delta\varepsilon$ lost by it in the PCI process can exceed E_1, i.e., $\Delta\varepsilon > E_1$. The energy of the slow scattered electron in the final state is then negative, and the electron may fall into an excited state in the discrete spectrum of the atom. The excitation functions for the discrete states then exhibit an oscillatory structure due to the increase in the probability that individual levels will be populated by the above mechanism (Fig. 2). Such structures have been observed for the excitation functions of He, Ne, and Ar.[1,6–8,10,53]

PCI effects in processes such as (1.6), i.e., in the photoionization of inner shells of atoms, have attracted considerable attention.[14–16,54–59] If the energy of the incident photon is much greater than the ionization potential of an inner vacancy, the photoelectron leaving the atom is slow. The motion of the slow photoelectron is significantly influenced by the field of the ion, which varies during the Auger-decay of the inner vacancy. Its energy decreases while the energy of the fast Auger electron increases. At the same time, the electron lines in the spectrum are both shifted and distorted, and this has been observed in the Auger-electron spectra corresponding to different Auger transitions, namely, $N_5 - O_{23}O_{23}(^1S_0)$ in Xe (Refs. 14, 54, 55, 57, and 59), $L_{23} - M_{23}M_{23}$ in Ar (Refs. 15 and 56), and $L_3 - M_4M_5$ in Xe (Ref. 58). The shift was investigated as a function of the incident-photon energy in Refs. 55–59 and as a function of the charge of the atomic nucleus in Ref. 54. An original method of investigating PCI by studying the Auger-line shift in the decay of the inner $2p_{1/2}$ vacancy in Se was used in Ref. 16. Photons of strictly defined energy were used to ionize the $2p_{1/2}$ shell of Se in different chemical compounds. This was used to vary the energy excess of the incident photon above the threshold in the shell under investigation in the range 1–7 eV.

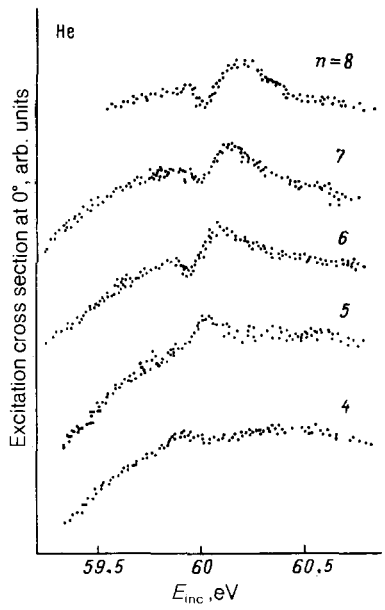

FIG. 2. Excitation functions for He by electron impact at 0° for Rydberg states with $n = 4$–8. Experimental data taken from Ref. 8.

We note that the observed shift and broadening of the lines were of the same order as the width Γ of the autoionizating state or the internal vacancy. The resolution of electron spectrometers is therefore usually of the order of a fraction of an electron volt.

The experimentally observed PCI effects were first interpreted on the basis of the classical Barker-Berry model.[4] This model was originally developed for ion-atom collisions, but was subsequently extended to the case of autoionization spectra excited by electrons.[1,5–7,60] The shift predicted by the model was in good agreement with experimental data well above the excitation threshold, but there was poor agreement for small differences between the energy of the incident particle and the excitation threshold. This discrepancy was readily explained by recalling that the model used in Ref. 4 was based on the classical description of particles leaving the event along rectilinear trajectories. The assumption breaks down for low velocities of the scattered particles.

The same point can be made about the eikonal approximation for which the range of validity is defined by (2.3). These conditions are definitely violated for low energies above the threshold. For example, for the photoionization process (1.6), condition (2.3) is equivalent to $E_1 \gg \Gamma^{2/3}$, where E_1 is the energy of the photoelectron. This inequality is violated for the intermediate atomic shells with $\Gamma \sim 0{,}1$–$0{,}2$ eV and photoelectron energies $E_1 \lesssim 1$ eV.

In the near-threshold region, we must therefore take into account the influence of the Coulomb field on the particle trajectories. This complicates the problem, but there is also a simplifying point. In very many cases, it may be considered that the velocity of the autoionization electron is high, and, in fact, higher than the velocity of the scattered particle in reactions (1.2), (1.5) or of the photoelectron reaction in (1.6) ($V_B \gg V_A$). It may therefore be considered that the autoionization electron rapidly leaves the reaction zone, so that its reaction with the slow particle can be neglected. When this is so, PCI reduces to the two-body problem in which the interaction of the slow particle A with the field due to the target ion, which varies in the course of the autoionization decay, must be taken into account.

The solution of this problem, i.e., the problem of de-

scribing PCI in the near-threshold region has been obtained for different models.[8,17–22,58] They are all based on the following general physical ideas:

(1) The velocity of the autoionization or Auger electron is assumed to be much greater than the velocity of the scattered particle or of the photoelectron, respectively. The interaction with the autoionization or Auger electron can be neglected, and PCI reduces to only the interaction between the slow particle and the field of the target atom, which varies in the course of the decay process.

(2) The slow electron or ion that is present near the excited target atom (ion) has no effect on the autoionization (Auger) decay probability, i.e., the decay occurs with the same width Γ and the same Lorentz energy distribution of emitted electrons as in the absence of the slow particle. The change in the distribution of emitted particles occurs exclusively as a result of their interaction with the field of the ion during the subsequent motion.

Process (1.5) can be conveniently investigated in the near-threshold region by the diagram techniques of the many-body theory.[61] The simplest graph describes the excitation of a single-particle autoionizating level by electron impact, followed by its decay (Fig. 3a). The thin line with arrow pointing right (left) describes the propagation of an electron (hole), whereas the line with the double arrow represents an electron in a discrete excited state; a wavy line represents the Coulomb interaction. Since the excitation and decay of a discrete state can proceed via virtual excitation of a particular atomic configuration, we must consider an effective interaction U instead of the Coulomb interaction, and represent the process by graph 3b in which the dashed lines represent the interaction U and the thick line of the discrete state indicates that the level width Γ has been taken into account. The analytic expression for the amplitude for the process represented by these graphs is

$$A_0(k_s) = \frac{\langle k_s, n|U|p, j\rangle\langle j, k_f|U|n, i\rangle}{\varepsilon_p - \varepsilon_s - E_{ex} + i(\Gamma/2)}, \qquad (3.2)$$

where E_{ex} is the AIS excitation energy and the remaining notation is clear from Fig. 3.

As noted above, the interaction between the slow electron of momentum k_s and the fast autoionization electron

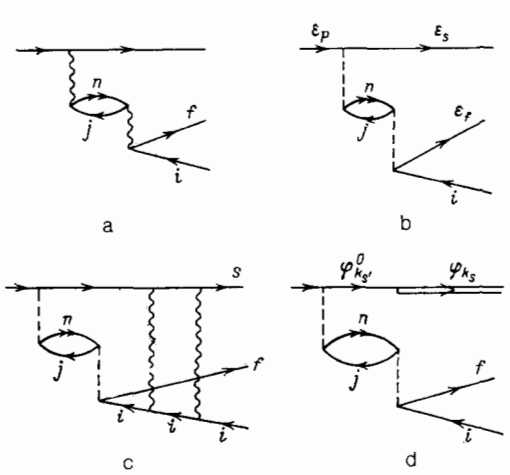

FIG. 3. Diagrams describing the processes of excitation by electron impact and decay of autoionization states and the post-collision interaction in the near-threshold region.

(momentum k_1) can be neglected in the near-threshold region in which $k_s \ll 1 \ll k_f$. PCI then reduces to the inclusion of the final-state interaction of the slow electron s with the hole i and with the field of the virtual autoionizing state n. If we use the well-known method presented in Ref. 62, the last interaction can be taken into account by introducing the appropriate Hartree-Fock wave function $\varphi^0_{k_s}$ of the slow electron in the field of the excited atom. The thin line corresponding to the slow electron in Fig. 3b represents its motion in this field. We must take into account the interaction of the slow electron and the vacancy i in the final state by summing the "ladder" of the diagrams such as those of Fig. 3c. Let $A(k_s)$ represent the sum of such graphs. We then have[21,63]

$$A(k_s) = \int A_0(k_s')\langle\varphi_{k_s}|\varphi^0_{k_s'}\rangle\, dk_s', \qquad (3.3)$$

where φ_{k_s} is the wave function of the slow electron in the field of the hole. This equation can be compared with the diagram of Fig. 3d in which the double line represents an electron moving in the field with the hole i, and the junction of the thin line with the double line represents the overlap integral $\langle\varphi_{k_s}|\varphi^0_{k_s'}\rangle$.

The amplitude (3.3) describes the instantaneous decay of the AIS for which the slow electron experiences a sudden change in the field. A similar method of taking into account the sudden change in the field is also valid for other processes in which a slow particle and an atom (ion) are produced in quasistationary states, e.g., in process (1.6).

Analysis of the amplitude given by (3.3) shows that the inclusion of PCI leads to a shift and a change in the shape of the autoionization line in the autoionization electron spectrum,[21,63] in complete agreement with the general properties of PCI discussed in Section 2. This is accompanied by a reduction in the energy of the slow electron and an increase in the energy of the fast electron. The autoionization line profile becomes asymmetric, the line declines more slowly than in the Lorentz case (without PCI) on the side of larger ε_f (smaller ε_f) and is steeper than the Lorentz line for small ε_f. Moreover, the broadening of one of the line wings is greater than the narrowing of the other. The net effect is that the line as a whole is broadened.

The reduction in the energy of the slow electron can be sufficient to ensure that it falls into a bound state, i.e., an excited atom is formed in the final state. In the case of inner-shell photoionization (1.6), the capture of the slow photoelectron to a bound final state of the reaction results in the formation of singly-charged ion in an excited state. The amplitude (3.3) can then be directly generalized to this case by taking for the wave function of the slow electron in the final state, φ_{k_s}, the corresponding function for the discrete state.[23]

Numerical methods and a computer have to be used to calculate the amplitudes and cross sections of particular processes on the basis of (3.3). Two approaches can be adopted in such calculations. In one,[21,48,58,64,65] the calculation is based directly on (3.3). A similar method has been used to calculate PCI effects for processes involving the excitation by electron impact of the $3s4p(^3P)$ autoionizing state in argon,[21,64] and for the scattering of a fast electron by argon when the energy ω transferred to the atom is close to the ionization threshold of the $2p^6$ shell and singly-charged ions Ar^+ are formed in the final state[65] [this process is analogous to the reaction (1.6), i.e., photoionization in the $2p^6$ shell,

followed by the capture of the slow photoelectron into a discrete state of Ar^+]. Another possibility is the photoionization of the L_3 shell of Xe, followed by the $L_3 - M_4M_5(^1G)$ Auger decay.[58] Figure 4 shows the results of such calculations and of measurements of the shift Δ of the autoionization $3s4p(^3P)$ line of argon. Figure 5 shows the density of generalized oscillator strengths corresponding to the cross section for the production of the singly-charged ions Ar^+, which takes into account the PCI effects. As can be seen, on the whole, this model provides a good description of the experimental data.[11,13]

This approach can also be used to take into account different correlation and relativistic effects. In the latter case, the intermediate-state wave functions were calculated as the eigenfunctions of the Dirac-Fock Hamiltonian.[48] This method was used to calculate the Auger line shapes and the shift of the Auger electron energy during the photoionization of inner shells and the subsequent Auger decays $K - L_2L_3(^1D)$ in argon and $L_2 - L_3L_4$ in xenon.[48]

In the other approach, the amplitude (3.3) was found by solving an inhomogeneous differential equation equivalent to (3.3). The solution of this equation under the corresponding boundary conditions is described in Refs. 68 and 69.

This method of finding the amplitude was also employed to investigate PCI during the photoionization of inner shells, followed by Auger decay.[66,67,70] A study was made of the shape of the Auger line profiles and of their positions in the spectrum in the case of the $L_{2,3}$ photoionization of argon[66,67,70] and of the Ns subshell of xenon.[67,70] Numerical calculations confirmed the strong effect of PCI on the shape and position of the Auger lines, in accordance with the general predictions of the theory. As an example, Fig. 6 shows the shape of the $L_3 - M_{23}M_{23}(S_0)$ line in argon (calculated with allowance for PCI). Figure 7 shows the shift of this line as a function of the energy excess E_1 of the incident photon.

Figures 6 and 7 also show the calculated line profile and the shift obtained within the framework of the eikonal theory.[23,40] The substantial discrepancy between these calculations, on the one hand, and the calculation reported in Ref. 67 and with experiment, on the other, confirms that the eikonal model is not valid in the near-threshold region in which conditions (2.3) are violated.

The PCI model known as the "shake-down" model[1,8] is based on the representation of the amplitude for the process by the overlap integral over the wave functions of the slow

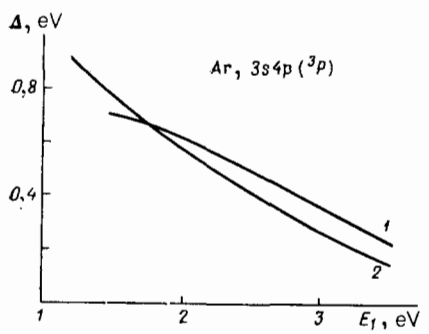

FIG. 4. Shift Δ of the $3s4p\ (^3P)$ autoionization line in Ar under excitation by electron impact as a function of the energy of the electrons E_1 above the excitation threshold. *1*—calculated,[21] *2*—experiment.[13]

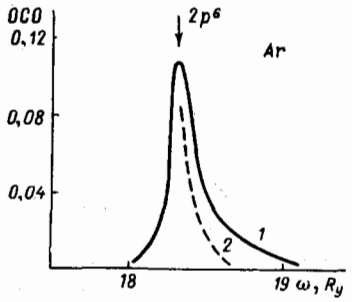

FIG. 5. Density of generalized oscillator strengths near the threshold for the ionization of the $2p^6$ shell of Ar as a function of the incident photon energy ω. *1*—calculated including the production of Ar^+ under the influence of PCI,[65] *2*—experiment.[11]

electron in intermediate and final states. Physically, this model assumes that the sudden removal of electrons from an inner shell is accompanied by a sudden change in the effective charge of the nucleus, which is experienced by the outer electrons.

The transition probability is determined by the overlap integral over the corresponding wave functions. The post-collision interaction is introduced in this approach within the framework of the shake-down approximation, discussed in detail in Ref. 3.

The shake-down model has been used to calculate the probability of capture of an electron to states with $n = 4$–8, $l = 0,1$ of the helium atom during the autoionization of the $2p^2(^1D)$ state of helium.[1,8] The dependence of this probability on the energy excess of the incident electron shows an oscillatory structure and can explain the experimental data.[6–8] This model was subsequently used[71] to calculate the probabilities of excitation of the autoionizing states $2s^2(^1S)$ and $2s2p(^3P)$ by electron impact in helium, which are found to be in agreement with experiment.[5] Analysis of the formulas developed in the shake-down model has shown[71] that they become identical with the formulas of the classical Barker-Berry model[4] in the limit of small energy shifts, i.e., large ε and small Γ.

The same idea of representing the amplitude for the process by the overlap integral over wave functions of the intermediate and final states is used as a basis for the popular semiclassical model.[19,20,22,44,47] As in the shake-down model, the normalized amplitude $A(E)$ for the process, for which

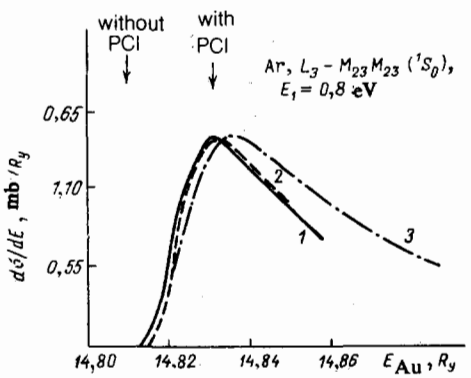

FIG. 6. Shape of the $L_3 - M_{23}M_{23}\cdot(^1S_0)$ line in the Auger spectrum of Ar for photon excess energy above the threshold $E_1 = 0.8$ eV. *1*—calculated including PCI and based on (3.3) from Ref. 67, *2*—calculated using the quasiclassical model, [20] *3*—calculated, eikonal approximation.[23]

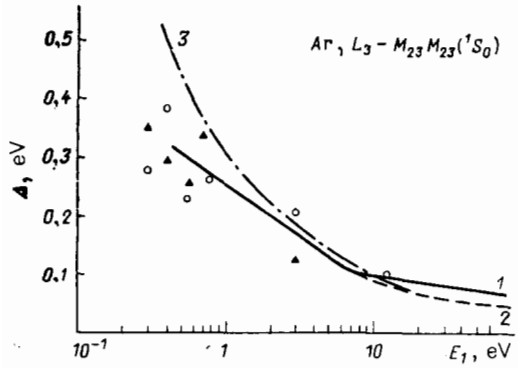

FIG. 7. Shift of the $L_3 - M_{23}M_{23}\cdot(^1S_0)$ Auger line in Ar as a function of the photon energy above the ionization threshold E_1. *1*—calculated,[67] *2*—calculated in the quasiclassical model,[20] *3*—eikonal approximation[23]; experiment.[15]

the particles exchange energy E as a result of PCI can be written in the form

$$A(E) = \left(\frac{\Gamma}{2\pi}\right)^{1/2} \langle \psi_i(\mathbf{r}, E) | \psi_f(\mathbf{r}, E) \rangle, \tag{3.4}$$

where ψ_i and ψ_f are the wave functions of the slow particle before and after the decay of the quasistationary state. In contrast to the shake-down model, here the WKB approximation is used for the wave functions (with a complex potential for the function ψ_i). Assuming that the quantities Γ, E, and r^{-1} are much smaller than the energy of the slow electron, the momentum of the particles can be expanded into a Taylor series and the amplitude (3.4) can be written in the form

$$A(E) = \left(\frac{\Gamma}{2\pi}\right)^{1/2} \int_0^\infty dt \exp\left\{-\int_0^t \left[\frac{\Gamma}{2} + i\left(E - \frac{1}{r(t')}\right)\right] dt'\right\}. \tag{3.5}$$

This integral is then evaluated by the method of stationary phase. The final expression allows for the fact that the amplitude may contain contributions due to different coherently excited intermediate quasistationary states as well as direct transitions. Effects connected with interference between these amplitudes will be discussed below in Section 6. The final result is that the probability of emission of an autoionization (or Auger) electron of energy ε_z is

$$P(\varepsilon_z) \sim \left| A + \sum_n C_n \exp(-i\alpha_n) \right|^2, \tag{3.6}$$

where A is the direct-transition amplitude. The sum over n takes into account all the possible intermediate coherent AIS.

The amplitudes C_n and phases α_n of the individual terms are given by (3.5) which can be evaluated by the method of stationary phase. They depend on the velocity of the scattered particle and the lifetime of the nth AIS. The precise form of these quantities is given in Refs. 12, 19, 20, and 38.

The other approach to the description of PCI within the framework of semiclassical theory is based on the consideration of the time-dependent transition amplitude.[19,20,72] The initial state is assumed to be a coherent mixture of different AIS, and relationships analogous to (3.5) can be obtained by representing the energies of the initial and final states by time-dependent potential curves. These approaches to the derivation of the formulas of the semiclassical PCI model are equivalent[20,24] because, although they use different mathematical formulas, they are based on the same physical ideas.

The semiclassical model has been used to obtain a simple relationship[20] for the energy transfer $\Delta\varepsilon$ between the fast and slow departing particles (i.e., the energy shift of the ionization electron) and the energy excess E_1 of the incident particle above the excitation threshold:

$$\Gamma[2(E_1+\Delta\varepsilon)]^{1/2} - 4\Delta\varepsilon(E_1+\Delta\varepsilon) - \Delta\varepsilon^2 = 0. \tag{3.7}$$

For small shifts, $\Delta\varepsilon \ll E_1$, the solution of (3.7) is given by the Barker-Berry formula (1.4) $\Delta\varepsilon_{BB} = \Gamma(8E_1)^{-1/2}$. However, in the near-threshold region, in which $\Delta\varepsilon \sim E_1$, the shift determined by the solution of (3.7) is significantly different from $\Delta\varepsilon_{BB}$. The expression given by (3.7) is simple and therefore particularly convenient for the interpretation of experimental data. The formulas of the semiclassical model have been used to analyze a large number of experimental spectra of autoionization and Auger electrons, and also excitation functions for processes (1.2), (1.5), and (1.6). This included the decays of the autoionizing states $2s^2(^1S)$, $2p^2(^1D)$, and $2s2p(^1P)$ in helium,[12,19,38,73,74] the $Ns - O_{23}O_{23}$ Auger decay in xenon,[14,20] and the $L_{23} - M_{23}M_{23}$ decay in argon.[15,22,56] As an example, Fig. 8 shows the shift $\Delta\varepsilon(E_1)$, calculated for N–OO Auger spectra in xenon. As before, this example illustrates the good agreement between experimental data and calculations based on the semiclassical model.

The alternative approach that generalizes the idea of the overlap integral was proposed in Ref. 18 and was based on the quasimolecular adiabatic theory. It has been used to solve the general problem of a slow quantum-mechanical particle interacting with a system that has a discrete state coupled to a homogeneous continuum. The transition amplitude obtained in this way involves the wave functions of the system in the intermediate state $a(\mathbf{R})$, the final state functions $\Phi_f(\mathbf{R})$, and the photoionization decay probability $\Gamma(\mathbf{R})$, which depend on the separation r between the slow particle and the atom:

$$A \sim \int d\mathbf{R} (\Gamma(\mathbf{R}))^{1/2} \Phi_f(\mathbf{R}) a(\mathbf{R}). \tag{3.8}$$

If we suppose that the width Γ in this relation is independent of $\mathbf{R}$, we find that (3.8) reduces to an overlap integral typical

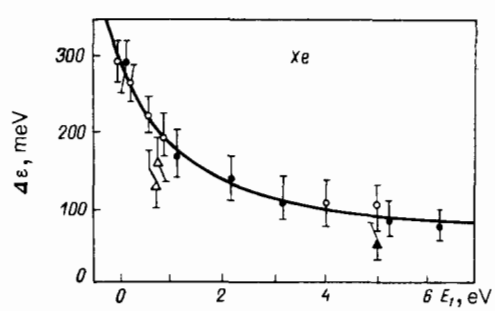

FIG. 8. Shift of the $N_5' - O_{23}O_{23}$ Auger line in Xe as a function of the energy of the photon above the ionization threshold. The calculation is based on the quasiclassical model[20] and the experimental data are taken from Refs. 14, 55, and 57.

for the shake-down models described above. By simplifying (3.8) still further, we can write $a(R)$ in the form $\exp(ikR)$, where the energy of the intermediate state is complex, i.e., $k^2/2 = E_1 - (i\Gamma/2)$, and the final-state functions $\Phi_f(R)$ are the Coulomb wave functions of the continuous (or discrete) spectrum. The resulting analytic formulas[18] for the amplitude and the cross section for the process are more general than those of Barker-Berry or shake-down models,[71] and can be used to analyze the contribution of the different factors to the formation of the autoionization line. For $E_1 \gg \Delta\varepsilon \gg \Gamma$ (E_1 is the energy of the incident electron above the excitation threshold and $\Delta\varepsilon$ is the energy transfer between the slow and fast electrons) we obtain the classical approximation and the resulting formulas become identical with those of the Barker-Berry formulas. When $\Gamma \gtrsim \Delta\varepsilon \gg (\Gamma/2V)^2$ eV (v is the velocity of the scattered electron), the autoionizing system must be described quantum-mechanically, and the scattering of particles associated with PCI can be described classically. In the region in which energy transfer is comparable with the energy of the slow particle, $\Delta\varepsilon \sim E_1$ and $(\Delta\varepsilon \lesssim (\Gamma/2V)^2$, the entire system must be described quantum-mechanically.

The formulas describing PCI effects have often been derived from very general quantum-mechanical ideas. The general formulas of the theory of scattering that generalize the theory of Feshbach resonances have been used to derive the scattering amplitude that includes both direct and resonance terms describing PCI.[17,48,75,76] The resonance amplitude that includes PCI effects has been derived from the two-potential formalism of Gell-Mann and Goldhaber in terms of complex coordinates.[77–80] These theories are based on different approaches, but the formulas that they produce are usually simplified for specific calculations and, in one way or another, reduce to the overlap integral (3.4). Integrals of this type are a central feature of practically all the PCI models for the near-threshold region that have been developed. Even in relatively coarse models, the evaluation of this integral is found to reproduce, if only qualitatively, the basic features of PCI. The success of any particular model that does not claim to provide a quantitative description of the effect normally relies on the more precise evaluation either numerically or analytically of the overlap integral.

4. THREE-PARTICLE EFFECTS

4.1. Experimental manifestations of predicted effects. Let us now examine specific manifestations of PCI that are due to the interaction between all three charged particles. They are particularly well-defined in (1.2), (1.5), and (1.6) when the velocities of the emitted particles are comparable in magnitude, i.e., $V_A \sim V_B \sim V_{AB}$. The distortion by PCI of the spectrum of reaction products in accordance with (2.7)–(2.10) depends on the single parameter ξ, given by (2.13). The two terms in this parameter represent, respectively, the interaction of particle A with the field of the ion and the interaction of particles A and B as they emerge from the reaction. The quantity ξ and, hence, the resultant PCI effect, are determined by the relative magnitude of these two terms with opposite signs. The velocity V_{AB} in the range $V_A \sim V_B$ that we are considering is very dependent on the angle at which particles A and B leave the reaction. Hence, ξ and, consequently, the PCI effect, show a strong dependence on the reaction kinematics. Depending on the velocities V_A, V_B and the angle θ_{AB}, the quantity ξ can be either positive or negative. This means that the shift $\Delta\varepsilon$ of the autoionization line (2.10) can also have either sign. The asymmetry of the line also depends on the sign of ξ and is determined by the factor $k(\xi,\varepsilon)$ (2.8). These effects depend on the three-body character of the problem, and do not manifest themselves in the region of near-threshold excitations discussed in Section 3.

We shall now discuss the experiments that have verified the theoretical predictions. In the case of reactions (1.5) and (1.6), there are two electrons in the final state. Coincidence experiments, in which the energy of the electrons and the angle between their velocities are measured, have to be carried out to determine the velocities that in turn determine the quantities $\xi, k(\xi,\varepsilon)$ in (2.8). Such experimental data on reactions involving three charged particles in the final state have not as yet been carried out, but they are expected in the near future.[81]

PCI effects are much easier to investigate in the case of ion-atom collisions (1.2). If the velocity of the ion is not too low, so that $V_I \sim 1$, there is a high probability that it will travel almost rectilinearly. Consequently, we need only measure the electron spectra for different angles β between the directions of the emitted electron and the incident beam. The theory outlined above predicts that the spectrum is very dependent on this angle (Fig. 9).[23,82] This result has a simple physical interpretation. For large angles between the emitted particles, the most significant factor is the repulsion between the scattered ion and the target ion, which leads to an increase in the energy of the former. For small angles, there is a large effect due to the attraction of the scattered ion to the electron, which reduces the energy of the ion. These predictions have been confirmed by recent experiments[43,83] that reveal a strong dependence of the position and profile of the autoionization electron lines on the emission angle β in collisions between ions Zi^{2+}, He^+, and He^{2+} with energies in the keV range and helium atoms. As an example, Fig. 10 shows the profile of the autoionization electron line emitted at 20° in collisions between Li^{2+} and helium, and the line is produced by exciting the $2s2p(^1P)$ AIS of helium. The line profile calculated from the eikonal theory [(2.7) and (2.8); Ref. 44] is in good agreement with experimental data.[43,83]

The other interesting manifestation of three-particle PCI effects in ion-atom collisions involves the dependence of the line shift $\Delta\varepsilon$ on the energy E_1 of the scattered particle. In the near-threshold energy range, the function $\Delta\varepsilon(E_1)$ is

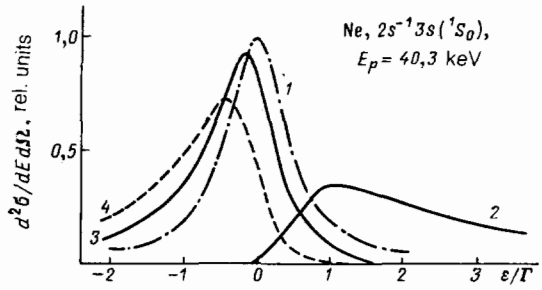

FIG. 9. Autoionization electron spectrum produced by excitation of the $2s^{-1}$ $3s(^1S_0)$ state of Na by proton impact.[23] ε is the energy measured from the unshifted value. *1*—without PCI, *2*, *3*—with PCI, *2*—$\beta = 15°$, *3*—$\beta = 120°$, *4*—Barker-Berry approximation.

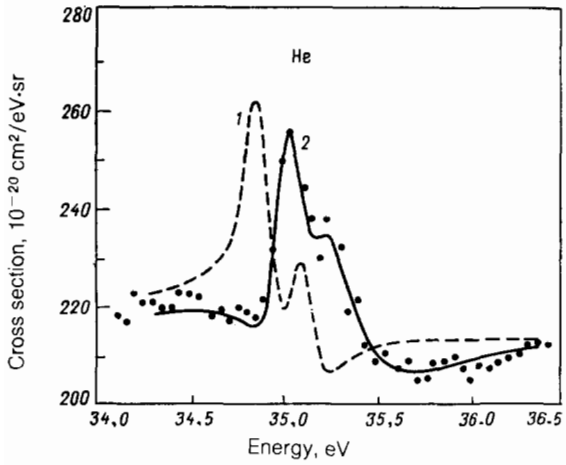

FIG. 10. Autoionization electron lines emitted at 20° during the decay of the 2s2p (^{1}P) state of He. The energy of the colliding particles in the system Li^{2+} + He is 700 keV. Calculations[44]: *1*—without PCI, *2*—with PCI, using the eikonal theory. The experimental points are taken from Refs. 43 and 83.

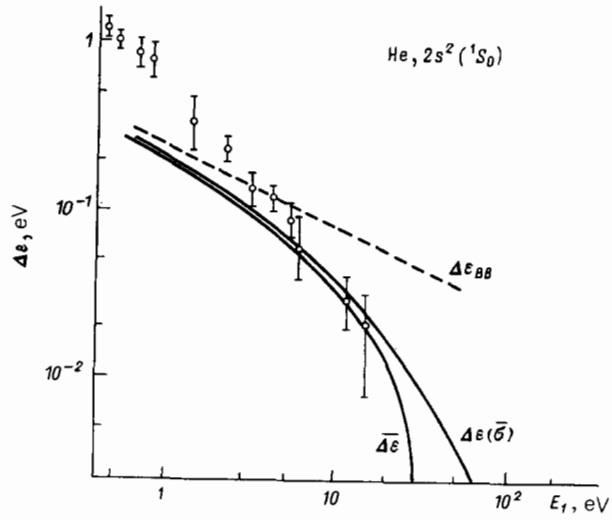

FIG. 12. Line shift in the spectrum of $2s^2(^1S_0)$ autoionization electrons in He under excitation by electron impact. E_1 is the energy of the incident electrons above the excitation threshold. See text for the definition of $\Delta\varepsilon$ and $\Delta\varepsilon(\bar{\sigma})$,$\Delta\varepsilon_{BB}$. Calculation—eikonal theory,[23] experimental points taken from Ref. 6.

monotonic and has the shape indicated in Fig. 8. In the region in which the velocities of the scattered ion and electron are comparable, the function is not monotonic and exhibits anomalous behavior. As an example, Fig. 11 shows the shift (2.13) calculated for the excitation of the $2s^{-1}3s(^1S)$ AIS in neon ($\Gamma = 95$ meV, $E_e^0 = 22.1$ eV). The anomalous behavior of the shift, shown in Fig. 11, has a simple physical interpretation. At low incident-electron energies, the PCI shift is determined by the repulsion between the scattered proton and the ion. The first term in (2.13) is then the dominant one, and the function $\Delta\varepsilon(E_1)$ has the usual profile observed in traditional near-threshold experiments. At high energies, the principal effect is due to the Coulomb attraction between the proton and the electron, which is very dependent on their relative velocity and produces the anomalous behavior of $\Delta\varepsilon(E_1)$.

We now return to reactions (1.5) and (1.6) with two electrons in the final state. Traditionally, PCI is investigated in such processes by a method in which the spectrum of only one (e.g., the autoionization electron) is examined. This spectrum is described by (2.7) after integration with respect to the emission angle of particle A. The shift of the autoionization line in these experiments can be estimated from the average shift $\overline{\Delta\varepsilon}$ given by (2.14), or from the average cross section $\Delta\varepsilon\ \overline{(\sigma)}$ (see Section 2). As an example, Fig. 12

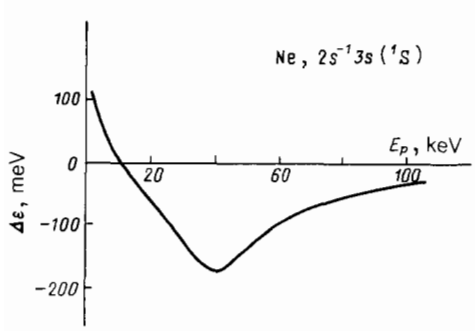

FIG. 11. Shift of the $2s^{-1}3s(^1S)$ autoionization line excited by proton impact in neon as a function of the incident-proton energy. Electrons emerging at 10°.

shows the shift $\Delta\varepsilon(E_1)$ of the autoionization line as a function of the energy excess E_1 of the incident electron above the $2s^2(^1S_0)$ AIS threshold in helium ($\Gamma = 138$ meV).[23] It follows from (2.14) and from numerical calculations that the energy shift of the autoionization line in the region in which $V_A \sim V_B$ is significantly smaller than the Barker-Berry shift $\Delta\varepsilon_{BB}$ (the latter is due to the strong interaction between electrons in this region). This fact was established by analyzing numerous experimental data.[41,75] On the whole, the shifts $\overline{\Delta\varepsilon}$ and $\Delta\varepsilon\ \overline{(\sigma)}$ that take into account the interaction of all three particles in the final state are in much better agreement with experimental data[6] than the Barker-Berry shift $\Delta\varepsilon_{BB}$.

The approximate nature of the shift ($\Delta\varepsilon$) given by (2.14), which does not take into account the dependence on the emission angles, is responsible for the "nontransmission effect" discussed recently in the literature.[24,41,46,59,84] If we consider the motion of the particle in the final state in terms of the classical model, the PCI effect does not appear at all when the velocity of the decay electron B is less than the velocity of particle A ($V_B < V_A$). The autoionization or Auger electron cannot then overtake the scattered particle and the latter does not experience the change in the Coulomb field. This fact is represented in (2.14) in which the PCI shift $\Delta\varepsilon$ is zero when ($V_B < V_A$). Evidence for this effect was obtained in the experiment reported in Refs. 59 and 84, but was probably due to inadequate energy resolution. When only one decay electron is recorded in the experiment, the corresponding line shift in the spectrum is described by the shift of the cross section (2.7) averaged over the angle Ω_A. Quantum mechanics shows that this shift $\Delta\varepsilon(\bar{\sigma})$ is small, but different from zero. This is illustrated by the calculations shown in Fig. 12. The "nontransmission effect" is therefore more likely to be due to the approximate character of the PCI model than to a real physical phenomenon. It is predicted by PCI models[24,46] that take into account the motion of the decay electron with an angle-averaged shift $\overline{\Delta\varepsilon}$, e.g., in the form given by (2.14).

4.2. Small relative velocities of emitted particles. So far, we have confined our attention to two energy ranges in which the PCI effects can be seen, namely, near-threshold excitation and the region in which the relative velocities of all three emitted particles are not small, but are comparable in absolute magnitude. There is one other interesting case in which the relative velocity of two of the particles is small and the velocity of the third is also small, i.e., $V_{AB} \ll 1, V_{AC} \approx V_{BC} \lesssim 1$. This occurs in reactions (1.2) and (1.5) when the excitation energy of the autoionizing state is low. Both the near-threshold excitations (A is the scattered particle with a low velocity $V_{AB} \ll 1$ relative to the ion) and the case where the scattered particle A and the autoionization electron B have equal and not very small velocities ($V_A \approx V_B \lesssim 1$) are investigated under these conditions. It is found that the problem can be solved analytically.[85]

When the condition $V_{AB} \ll 1$ is satisfied, the pair A – B interacts for a long time and its Coulomb interaction energy is high. This interaction must therefore be taken into account exactly. The interaction with the third particle cannot be taken into account by perturbation theory because the parameters $e^2/\hbar V_{AC} \approx e^2/\hbar V_{BC} > 1$ are large, but it can be allowed for within the framework of the eikonal approximation. Overall, the emission picture is as follows. The strong interaction between particles A and B, which persist for a long time, produces a significant distortion of their trajectories, which are not rectilinear. The interaction with the third particle is also large, but occurs at large distances and has only a slight effect on the trajectory of the pair A – B. It is this that justifies the application of the eikonal approximation. In other words, the conditions for the eikonal approximation (2.3) are satisfied in this case for the interacting pairs A – C and B – C, but the eikonal condition is violated for the pair A – B. Instead, the authors of Ref. 85 considered the less stringent restriction on V_{AB}:

$$(m_A+m_B)V_{AB}V_{AC} \gg (|z_A|+|z_B|)|z_C|R^{-1}, \tag{4.1}$$

where R is given by (2.1).

When (4.1) is satisfied, the amplitude for (1.1) can be written in the form[85]

$$M = M_1 M_2 \left(\varepsilon + i\frac{\Gamma}{2}\right)^{-1} S, \tag{4.2}$$

where M_1, M_2, and ε are defined above (Section 2) and the factor S is given by the following expression for $V_{AB} \ll 1$:

$$S = e^{-\pi\xi_0/2}\Gamma(1+i\xi)\left(\varepsilon + i\frac{\Gamma}{2}\right)^{-i\xi}\left(\frac{k_{AB}\varkappa}{\mu_{AD}} + \mathbf{k}_{AB}\mathbf{V}_{AD}\right)^{i(\xi_{AC}-\xi_{AD})}$$
$$\times\left(\frac{k_{AB}\varkappa}{\mu_{AD}} + \mathbf{k}_{AB}\mathbf{V}_{AD} + \varepsilon + i\frac{\Gamma}{2}\right)^{i(\xi_{AB}-\xi_{AC}+\xi_{AD})} \tag{4.3}$$

The quantities ξ_{ij}, ξ in this expression are given by (2.9), the relative momentum is $\mathbf{k}_{AB} = \mu_{AB}\mathbf{V}_{AB}$, μ_{ij} is the reduced mass of the pair i, j, and the momentum of the relative motion of A, D in the intermediate state is $\varkappa = \{2\mu_{AD}[\varepsilon_0 + i(\Gamma/2)]\}^{1/2}$. If the relative velocity V_{AB} is not too low, so that the eikonal condition (2.3) is satisfied for the A – B interaction, the expression given by (4.2) reduces to the eikonal expression (2.4).

The general expressions given by (4.2) and (4.3) can be used to calculate the cross sections for special cases of (1.2), (1.5), and (1.6). They were used in Ref. 85 to calculate the profile of the $3s^{-1}4p(^1P)$ autoionization line in argon excited by electron impact. The low energy of the autoionization electron, $E = 10.85$ eV, means that the line profile must be described with allowance for the interaction between the slow scattered electron and the field of the ion. The calculation is illustrated in Fig. 13 for the scattered-electron energy of 0.4 eV, and shows that the contribution of the interaction between the electrons in this process is very significant even against the background of the strong interaction between the slow electron and the field of the ion.

Allowance for PCI by means of (4.2) and (4.3) in the range $V_{AB} \ll 1$ can also be very significant in processes involving the capture of an electron into the continuum by the incident ion.[86]

5. REACTIONS WITH FOUR CHARGED PARTICLES IN THE FINAL STATE

We now turn to resonance processes in which the final state contains four charged particles. They include inner-shell ionization by electron or ion impact, followed by the Auger decay of the inner vacancy [reactions (1.7) and (1.8)]. Experiments on PCI effects in these reactions are much more diverse than those in the case of (1.1). The phenomenon can be studied in different coincidence experiments, the role of kinematics in PCI effects can be investigated, and so on. Two charged particles, namely, the scattered particle and the electron ejected from the inner shell, are produced as a result of inelastic collision between the incident particle and the target atom in which the latter is ionized. These particles move in the field of the excited ion prior to decay, and in the field of the ion and the Auger electron after the decay. In contrast to (1.1), PCI is then due to the interaction between the two charged particles, on the one hand, and the quasistationary particle and its decay products, on the other. The strength and character of this interaction depend significantly on the relative velocity of the scattered particle and the electron ejected from the atom. Allowance for PCI is therefore divided into two stages. First, we have to estimate the interaction between the four charged particles in the final state of (1.7) and (1.8) for particular fixed velocities (or energies) of the scattered particle and electron ejected from the atom. Second, we have to allow for the probability of a particular sharing of the energy of the incident particle between the scattered particle and the ejected electron. This probability is determined by the inelastic scattering that gives rise to the ionization of atom, and is not the subject of the PCI investigation. However, the energy distribution among the emitted particles has a significant influence on the magnitude of the PCI effect and must be taken into account when the latter is investigated.

The exact solution of the PCI problem in processes such as (1.8), which is valid in a wide range of relative electron velocities, can be obtained in the eikonal approach.[32] The interaction between the particles contributing to PCI is usually significant only for large separations (see Section 2). It may therefore be considered that the potential energies of interaction between the scattered electron (e_1) and the ejected electron (e_2), with the field of the ion, and also with the Auger electron (e_3) are less than the kinetic energies of the electrons. We shall also assume that the angles between the directions of the electrons are not small. If this is so, then the

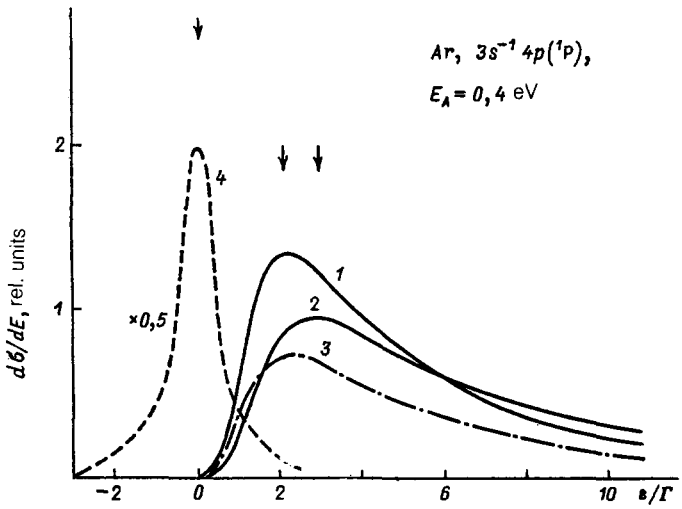

FIG. 13. The $3s^{-1}4p(^1P)$ autoionization line profile in Ar under excitation by electron impact.[85] Scattered-electron energy 0.4 eV. *1*—PCI with allowance for the interaction of three particles in the final state, *2*—the interaction of only the two slow particles taken into account, *3*—eikonal approximation, *4*—result obtained without taking PCI into account.

electrons travel almost uniformly and rectilinearly at large distances, which guarantees the validity of the eikonal approximation. The problem of four charged particles is then hardly more complicated than the three-particle problem examined in Section 2. More than that, the cross section for process (1.8) is given by an expression that is almost exactly the same as (2.7)[32]:

$$\frac{d^8\sigma}{dE_1 dE_3 d\Omega_1 d\Omega_2 d\Omega_3} = \sigma_0(E_1, \Omega_1, \Omega_2)\frac{\Gamma_{Au}}{2\pi[\varepsilon^2 + (\Gamma^2/4)]}k(\xi, \varepsilon). \tag{5.1}$$

where ε is the energy of the Auger electron E_3, measured from its unshifted position E_0^3: $\varepsilon = E_3^0 - E_3$, Γ_{Au} is the partial width of the Auger decay, and σ_0 is the ionization cross section of the inner shell of the atom by electron impact, which depends on the energies and emission angles of electrons e_1 and e_2. The factor $k(\xi,\varepsilon)$ that describes the PCI effects has already been encountered in (2.8). The only significant change is in the main parameter of the theory, which now takes the form

$$\xi = \left(\frac{1}{V_{13}} - \frac{1}{V_1} + \frac{1}{V_{23}} - \frac{1}{V_2}\right)\frac{e^2}{\hbar}. \tag{5.2}$$

The individual terms in (5.2) describe the interaction between electrons e_1, e_2 and the products of the Auger decay e_3, A^{2+}.

The cross section (5.1), regarded as a function of the energy ε, describes the shape of the Auger line, subject to the condition that the velocities of the emitted particles $\mathbf{V}_1$, $\mathbf{V}_2$, $\mathbf{V}_3$ are determined in the final state. Because of energy and momentum conservation, the cross section is then determined by eight independent parameters, e.g., the energies E_1, E_2 and the electron emission angles Ω_1, Ω_2, Ω_3. As in the case of (1.1), the shift of the cross section (5.1) is determined exclusively by the parameter ξ:

$$\Delta\varepsilon = \frac{\xi\Gamma}{2}. \tag{5.3}$$

The expressions given by (5.1), (5.2), and (5.3) show that all the PCI manifestations are very dependent on the kinematics of the emitted electrons.

Triple-coincidence experiments are necessary if this dependence is to be observed. However, such experiments have not yet been carried out, but there have been recent experiments in which two electrons, namely, the scattered and the Auger, or the scattered and the ejected electrons, were recorded in coincidence.[28,29,90,91] To describe this cross section, we must integrate (5.1) over all the directions of, say, the ejected electron:

$$\frac{d^8\sigma}{dE_1 dE_3 d\Omega_1 d\Omega_3} = \int d\Omega_2 \frac{d^8\sigma}{dE_1 dE_3 d\Omega_1 d\Omega_2 d\Omega_3}. \tag{5.4}$$

Estimates and calculations show[32] that the cross section (5.4) can often again be represented by (5.1) with the parameter ξ replaced with its average $\bar{\xi}$ evaluated over the angles Ω_2:

$$\bar{\xi} = \frac{1}{4\pi}\int d\Omega_2 \xi = \frac{e^2}{\hbar}\left(\frac{1}{V_{13}} - \frac{1}{V_1} + \begin{cases} 0, & V_2 \geqslant V_3, \\ \dfrac{1}{V_3} - \dfrac{1}{V_2}, & V_3 \geqslant V_2 \end{cases}\right). \tag{5.5}$$

As an example, Fig. 14 shows the $L_2 - M_{23}M_{23}(^1P)$ line in argon, calculated in this way and corrected for the detector transmission function. As can be seen, there is good agreement between calculations and experiment.[29]

It is interesting to note that double coincidence experiments can provide complete information about the cross section (5.1) if we consider inner-shell ionization by ion impact, i.e., processes such as (1.7). The above theory can readily be extended to this case, and the cross section and shift are then again described by (5.1)–(5.3), except that now the index 1 refers to the scattered ion. If we suppose that the ion travels almost rectilinearly at high enough energies, complete information about the process can be obtained from coincidence experiments in which measurements are made of the energy and the direction of emission of the ejected and Auger electrons. The feasibility of such experiments has been confirmed.[28,29,90,91]

The other possibility is to investigate (1.7) in coincidence experiments in which the energy of the scattered ion and the energy and direction of emission of the Auger electron are recorded. If we investigate the energy range in which the energy of the Auger electron is significantly greater than the energy of the ejected electron, i.e., $E_3 \gg E_2$, the parameter ξ is no longer a function of Ω_2, but is given by

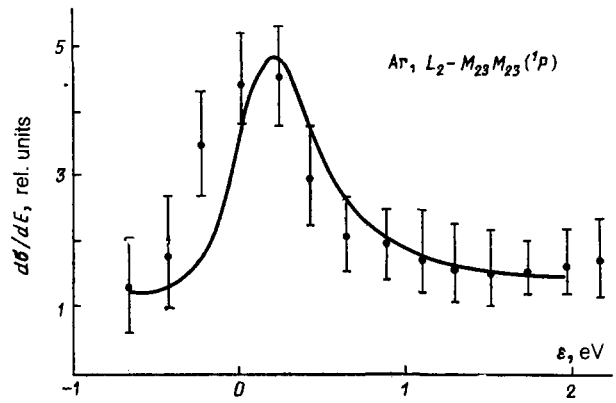

FIG. 14. $L_2 - M_{23}M_{23}(P)$ line profile in the Auger spectrum in Ar using coincidences between the scattered and Auger electrons. ε is the electron energy measured from the unshifted value. Calculation based on the eikonal model,[32] experimental points taken from Ref. 29.

$$\xi_{\text{ion}} \approx \bar{\xi}_{\text{ion}} = \frac{e^2}{\hbar}\left[Z_1\left(V_1^{-1} - V_{13}^{-1}\right) + V_3^{-1} - V_2^{-1}\right], \tag{5.6}$$

where Z_1 is the charge of the ion. The cross section recorded in such experiments is given by

$$\frac{d^4\sigma}{dE_1 dE_3 d\Omega_3} = \frac{\Gamma_{\text{Оже}}}{2\pi\left[\varepsilon^2 + (\Gamma^2/4)\right]} k\left(\bar{\xi}_{\text{ion}}, \varepsilon\right) \times \int \sigma_0\left(E_1, \Omega_1, \Omega_2\right) d\Omega_1\, d\Omega_2. \tag{5.7}$$

Its shift is

$$\Delta\varepsilon_{\text{ion}} = \frac{\bar{\xi}_{\text{ion}}\Gamma}{2}. \tag{5.8}$$

The dependence of this shift on the incident-ion energy has the anomalous nonmonotonic character found for processes with three particles in the final state.

As an example, Fig. 15 shows the shift of the $N_5 - O_{23}O_{23}(S_0)$ Auger line in xenon excited by proton impact. The anomalous form of the function $\Delta\varepsilon_{\text{ion}}$ is due to the strong attraction between the scattered ion and the Auger electron in this region, in which their relative velocity is small.

We now return to the ionization of atoms by electron impact (1.8). Extensive data on the Auger line shift as a function of the incident-electron energy E_0 have been obtained in experiments in which only one Auger electron

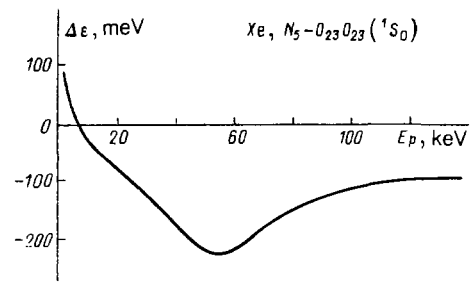

FIG. 15. The $N_5 - O_{23}O_{23}$ Auger line shift in Xe under excitation by proton impact. Energy of ejected electrons 5 eV, angle of emission of Auger electrons 10°. The dependence on the proton energy E_p is calculated from the eikonal theory.[32]

emitted at a particular angle to the incident beam was determined. Such measurements have been carried out for a number of Auger transitions from the $K_1L_{2,3}$ shells of argon,[30,31,92–97] the K shell of neon,[26,92,97] the $N_{4,5}$ subshells of xenon, and the M_{23} and M_{25} subshells of krypton.[25,27,99] The Auger-electron distribution measured in such experiments can also be described by (5.1), integrated with respect to the angles of the ejected and scattered electrons, and also with respect to the scattered-electron energy. The shift of the Auger line is now determined by the position of the maximum of this integrated cross section. This occurs at the energy $\tilde{\varepsilon}$ that is the root of the equation[32]

$$\frac{2\tilde{\varepsilon}}{\Gamma} = \frac{\int_0^{E_0 - I} dE_1 \int d\Omega_1 d\Omega_2 \xi\sigma_0 k\left(\tilde{\varepsilon}, \xi\right)}{\int_0^{E_0 - I} dE_1 \int d\Omega_1 d\Omega_2 \sigma_0 k\left(\tilde{\varepsilon}, \xi\right)}. \tag{5.9}$$

A rough estimate for $\overline{\Delta\varepsilon}$ can then be obtained by averaging the expression for the shift of the triple differential cross section (5.3) over all the angles and energies of the incident and scattered electrons:

$$\overline{\overline{\Delta\varepsilon}} = \frac{\Gamma}{2}\frac{\int \xi\sigma_0 d\Omega_1 d\Omega_2 dE_1}{\int \sigma_0 d\Omega_1 d\Omega_2\, dE_1}. \tag{5.10}$$

To determine the shift in accordance with (5.9) and (5.10), we must know the form of the cross section $\sigma_0(E_1, \Omega_1, \Omega_2)$ or the form of the energy distribution among the scattered electron (E_1) and the ejected electron (E_2). This is a problem that is well outside the framework of the present review.[100] The Auger line shift was calculated in Ref. 32 for a number of shells of inert gases, and the ionization cross section was described by the formulas of the symmetrized binary theory.[101] Good agreement with experimental data (Fig. 16) can be achieved by calculations of this kind, based on (5.9) and (5.10).[32] Comparison with calculations based on other models[31,41,87] shows that it is important to take into account the interactions between all the charged particles in the final state when the PCI shift is calculated, and correct

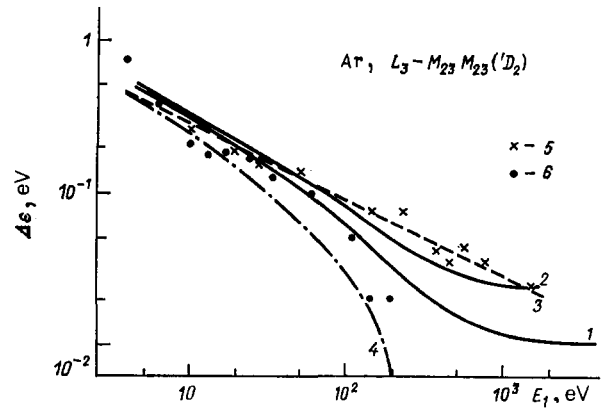

FIG. 16. The $L_3 - M_{23}M_{23}(^1D_2)$ Auger line shift in Ar as a function of the energy excess E_1 of the incident electrons above the threshold. *1*—calculated from (5.9) [Ref. 32], *2*—calculated from (5.10) [Ref. 32], *3*—model calculation,[31,87] *4*—model calculation[41]; experiment: *5*—Ref. 93, *6*—Ref. 92.

allowance has to be made for the distribution of energy among the scattered and the ejected electrons.

The characteristic feature of the shift calculated from (5.9) and (5.10) is its behavior at high incident-electron energy E_0. In contrast to the model calculations reported in Refs. 41 and 87, the magnitude of the shift is then constant and nonzero. The finite shift at high energies is readily explained. Even when the energy excess of the incident electron above the threshold is high, there is an appreciable probability that electron E_2 will have a low velocity. The interaction of this low-energy electron with the Auger-decay products leads to energy exchange with the Auger electron, i.e., to a shift of its line in the spectrum. Measurements of the energy of the Auger electrons emitted as a result of photoionization and ionization of atoms by electron impact will therefore yield different values even in the limit of high energy excess above the ionization threshold. The energy of Auger electrons produced by photoionization is lower than the electrons released in ionization by electron impact.

The behavior of the shift for high incident-particle energy E_0 has also been investigated in terms of the semiclassical model,[33,97,102] using the expression for the shift obtained in an implicit form in the model described in Ref. 24, which takes into account the interaction between the emitted electrons and the Auger electron. The shift was averaged with allowance for the energies of the scattered and ejected electrons E' and E''. The energy distribution was examined in the first Born approximation and was subsequently expressed in terms of the Bethe approximation.[103] The values of $\Delta\varepsilon(E_0)$ obtained in this model are in good agreement with experimental shifts for the $K - L_{23}L_{23}$ transitions in argon and neon.[97]

Analysis of the expression obtained in this way has shown[33] that the shift tends to a positive constant for asymptotically large energy excess above the ionization threshold. The asymptotic shift can be estimated from the expression[33,102]

$$\Delta\varepsilon_{as} \approx \frac{V\overline{\pi}\,\Gamma}{2\,(2E_B)^{1/2}} \text{ (at. units)}, \tag{5.11}$$

where E_B is the energy of the initial vacancy. More accurate numerical calculations of the asymptotic shift were carried out using the Hartree-Fock wave functions for a number of inner shells in neon, argon, and krypton. The differences between the values obtained in this way and the results reported in Ref. 32 are probably due to the approximate character of the electron energy distributions used in the models.

Since the asymptotic shift is small (tens or hundredths of meV, it is difficult to measure. Nevertheless, there is recent experimental evidence[96,97,104] that the Auger line shift is constant at high electron energies.

We shall now review other papers devoted to the theory of PCI in reactions with four charged particles. One of the assumptions is that the scattered and ejected electrons travel equal energies in opposite directions.[31,41,87,88] This assumption is particularly well founded in the near-threshold region in which the energy excess of the incident electron above the ionization threshold E is found to be zero, and the well-known Wannier regime is established.[89] The interaction with the fast Auger electron is now unimportant and a classical analysis of emission kinematics can be used to describe the energy distribution of the Auger electron and its shift.[31,87] The equipartition of energy among the electrons has been used[14,87,88] to estimate the shift $\Delta\varepsilon$ for the Auger electron.

Since, for high excess energy E, the velocities of the emitted particles are comparable in magnitude with the velocity of the Auger electron, their interaction must be taken into account in PCI. This has been done in the classical model[41] that takes into account the finite velocity of the Auger electron and the time of its emission from the atom. This led to the following relationship for the Auger-electron line shift $\Delta\varepsilon$, the energy excess above the ionization threshold E, the width of the inner vacancy Γ, and the unshifted Auger electron energy E_A^0:

$$\frac{\Delta\varepsilon}{\Gamma} + (E_A^0)^{-1/2} = E^{-1/2}. \tag{5.12}$$

It is clear that the shift $\Delta\varepsilon(E)$ given by this expression is actually the lower limit, since it is based on the assumption of equipartition of energy among the scattered and ejected electrons.

In reality, the energy is arbitrarily shared between the scattered (E') and ejected (E'') electrons. An attempt to take this into account for high values of E was undertaken in Ref. 31 in which it was assumed that the total energy shift of the Auger electron was the sum of the shifts determined by the interaction of each of the electrons E', E'' with the field of the ion: $\Delta\varepsilon = \Delta\varepsilon(E') + \Delta\varepsilon(E'')$. These shifts, in turn, were determined from formulas such as the Barker-Berry formula (1.4) for high E', E'', or the Niehaus formula (3.7) [for small E' and negligible $\Delta\varepsilon(E'')$]. The shifts obtained in this way were then averaged over the Born distribution $d\sigma/dE'$ of the energies E',E'' ($E' + E'' = E$). The $L_{23} - M_{23}M_{23}$ line shift in argon was thus calculated for a number of incident-electron energies.[31] Despite the large number of approximations, the results obtained in this way are in reasonable agreement with experiment.[31]

6. INTERFERENCE EFFECTS

So far, we have confined our attention to resonance processes such as (1.1) that involve the excitation of only one intermediate autoionizing state D. Direct processes such as (1.9) also contribute to the electron spectrum. Since the final states in these reactions are coherent, the total amplitude includes the sum of the amplitudes for resonance and direct processes. The amplitude for the direct process (1.1) is a smooth function for energies $\sim\Gamma$ in the neighborhood of the autoionization line. When the PCI effect is not included, the phase of the resonance amplitude [see, for example, (3.2)] changes by π in the region of the resonance, so that the cross section assumes the characteristic Fano profile. When PCI is included, this has a considerable effect on the change in the phase of the resonance amplitude.[18,19,21] The correction to the phase becomes very significant when the relative velocity of any pair of particles,e.g., V_{AB} is small ($V_{AB} \ll 1$). This is clear from (4.3) in which $\arg\Gamma(1 + i\xi)$ undergo a considerable change even for small change in V_{AB}. The smaller the velocity V_{AB}, the greater this change. This is due to the fact that the Coulomb forces have a long tail. The phase change can reach $\sim\pi$ or more as the energy ε varies over the width $\sim\Gamma$ if the following condition is satisfied:

$$\mu_{AB}V_{AB}^3 < \Gamma. \tag{6.1}$$

Each increment of π in the phase leads to an additional peak and a minimum in the cross section, so that the latter exhibits an oscillatory structure.[18,21,63] This has been carefully investigated for near-threshold excitations in processes such as (1.2), (1.5), and (1.6).[18,19,63] It is clear from (6.1) that the oscillation effect is difficult to observe in the case of heavy-particle collisions for which $\mu_{AB} \gg 1$.

We shall now consider the case where an inelastic collision $X + Y$ results in the excitation of not only D, but also other autoionizing states D′, D″, etc. If the decay channels for these states coincide, and the excitation energies are close to one another, the spectrum of the reaction products in (1.1) will reflect the possibility of excitation and decay of the different autoionizing states (D, D′, D″), etc. In other words, by recording the energy and the emission angle of the autoionization electron or of the scattered particle in coincidence (or noncoincidence) experiments, we can identify events involving both the excitation of the state D and the excitation of close autoionizing states D′, D″,... . Since the final states in all these processes are coherent, the spectrum of the reaction products can be described by an amplitude that is the sum of the amplitudes for the individual processes. Interference between these amplitudes can then lead to the appearance of oscillations in the observed spectrum. Such oscillations were first observed in the spectrum of autoionization electrons in collisions between He^+ ions and helium atoms.[12] The close autoionization states $2s^2(^1S)$,$2p^2(^1D)$, and $2s2p(^1P)$ provided a contribution to the spectrum.

In addition to processes (1.1) that proceed via the excitation and decay of AIS, nonresonance processes such as (1.9) contribute to the electron spectrum. The total amplitude for the production of electrons of given energy ε_2 includes the sum of the amplitudes for the resonance and direct processes[19]:

$$P(\varepsilon_2) \sim \left| A + \sum_n C_n \exp(-i\alpha_n) \right|^2. \qquad (6.2)$$

Each term in the sum over n corresponds to the excitation of a specific AIS, and the amplitude A describes the direct process (1.9). The amplitudes C_n and phases α_n represent the PCI effect and can be expressed by formulas such as those, for example, provided by the semiclassical model.[19] These amplitudes contain as factors the amplitudes describing the probability of excitation of a particular AIS (D, D′, D″, etc). Their moduli and phases can be regarded as adjustable parameters when model calculations are compared with experimental data.[12,72,73] This also applies to the modulus and phase of the direct amplitude A (Refs. 19 and 38). It is important to note that the interaction between the particles in the final state affects the amplitude A for the direct process. This interaction has been investigated by a number of workers (see, for example, Refs. 34–36), but such studies have not extended to PCI and lie outside the framework of the present review. At any rate, the inclusion of this interaction does not affect the smooth character of the amplitude A in the resonance region. Comparison between experimental data and the spectrum calculated from (6.2) has led to information about the AIS excitation probability[19,38,73] and has also been used to investigate the degree of coherence in the excitation of different AIS.[71,74]

Interference between the amplitudes for the PCI effects in the spectrum of photoionization electrons has been investigated during the excitation of AIS by ion impact,[12,19,72,73,105,114] by electron impact[19,38,71,74] and by photoionization of inner shells.[20] As an example, Fig. 17 shows the autoionization-electron spectra obtained in e + He collisions. The interpretation of these data in terms of (6.2) was bssed on the assumption of interference between the $2s^2(^1S)$ and $2s2p(^3P)$ resonance states of helium and the direct process.[19] A similar analysis was used to explain the oscillatory structure of the excitation functions of Rydberg states populated by the PCI mechanism in reaction (1.8).[19] On the whole, the use of (6.2), which takes into account PCI effects in the semiclassical model, and variation of the adjustable parameters, have led to a successful description of a large set of experimental data on the spectra of autoionization electrons, scattered particles, and excitation functions of Rydberg states.[19]

Manifestations of interference effects in electron spectra and the influence of PCI upon them depend on the method of observation. If all electrons emitted at a particular angle Ω in ion-atom collisions are recorded, it is found that PCI has generally no effect on the character of the interference spectrum.[39] The total electron intensity $I(\Omega)$ is then independent of the velocity of the colliding particles and is determined exclusively by the probabilities of excitation of the close autoionizing states D_1 and D_2, their decay widths Γ_1, Γ_2, and the nominal-energy difference $\Delta\varepsilon^0$ between the ionization electrons produced in the decay of these states. The shape of the differential (in energy) spectra $I(\Omega, E_e)$ is highly distorted by the PCI effects described above.

We have already noted that PCI has an important effect on interference between direct (1.9) and resonance (1.1) amplitudes for low relative velocities of charged particles emerging from the reaction ($V_{AB} \ll 1$).[106] These effects can be observed, for example, when an electron is captured by an

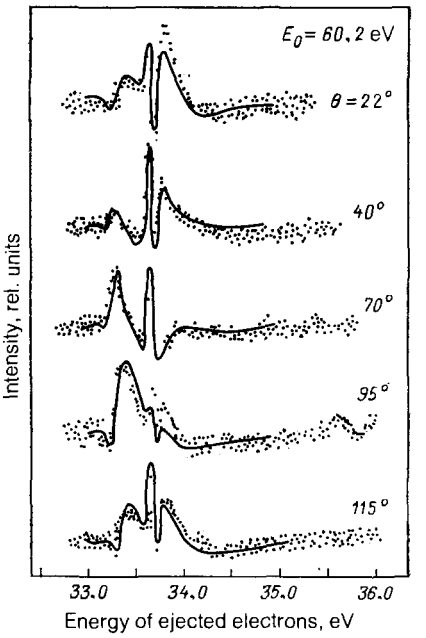

FIG. 17. Interference effects in the autoionization electron spectrum produced in e + He collisions. Incident-electron energy $E_0 = 60.2$ eV. The angles of emission of the autoionization electron are indicated in the figure. The calculations were based on the quasiclassical theory,[19] taking into account the contribution of direct processes and also of the $2s^2(^1S)$ and $2s2p(^3P)$ states. The experimental points were taken from Ref. 5.

ion into a continuum state.[86] The characteristic cusp in the cross section for the direct process[86] is then distorted by the oscillatory structure due to the interference. The observability of these predicted effects is very sensitive to the angle between the emitted particles.[106]

7. CONCLUSION. UNRESOLVED PROBLEMS

It is interesting to follow from the modern standpoint, the evolution of ideas on the post-collision interaction. The phenomenon was discovered experimentally as a near-threshold effect in ion-atom collisions. The early intuitive ideas were then extended to the electron-atom and photon-atom collisions. This was followed by a rapid development of the theory of the phenomenon in the near-threshold region. Considerable advances were made when the following three facts were understood: (1) the phenomenon is not confined to the near-threshold region, (2) it is essentially a three-particle problem, and (3) a parametrically exact solution of the three-particle problem can be obtained. The recognition of these facts led to a new view of the entire problem of post-collision interaction and has resulted in a better description of the reactions with four charged particles in the final state.

In the preceding Sections, we have described the principal effects due to the post-collision interaction in the spectra of the products of resonance processes. All these effects, including line shifts, distortion of line profile, shift of the ionization threshold, capture of the ejected electron, and interference between the amplitudes for direct and resonance processes are, on the whole, satisfactorily described by existing models of PCI. Theories developed in the course of the last few years are also capable of predicting different three-body PCI effects in the spectra of reaction products.

On the other hand, experimental studies of PCI have largely been confined to the near-threshold energy range in which three-body effects are not observed. Individual experiments that record the presence of PCI effects outside the near-threshold region are clearly inadequate. It would therefore be desirable to have systematic experimental studies of the phenomenon in the region in which the relative velocities of emitted particles are comparable in magnitude, and three-body effects can be observed.

The most interesting and immediate tasks for experimenters appear to be the following.

(1) Measurement of the dependence of the line shift and asymmetry on reaction kinematics, i.e., on the emission angles and relative velocities, including the sign of the shift and the line asymmetry.

Different types of experiments, can be carried out depending on the type of reaction employed. (1.1). If the incident particle is an ion, a noncoincidence experiment can be carried out. (1.2) A coincidence experiment is necessary for (1.5) and (1.6), and the decay and scattered (or photo) electrons are recorded in coincidence. It is important to note that the experiments performed so far have been confined to the dependence of the line profile on the kinematics of reaction (1.2).[43,83,105]

2. For reactions with four charged particles, e.g., (1.7) and (1.8), the PCI experiments can be even more diverse. (2.1). The most complete experiment will involve measurements of coincidences between the three particles in the final state and the verification of predictions based on (5.1). (2.2). The dependence of line profiles and positions on reaction kinematics can be investigated by recording two charged particles in coincidence, namely, the scattered and the Auger electrons, or the scattered and the ejected electrons. (2.3). In the "noncoincidence experiment," in which only one Auger electron is recorded, the interesting and subtle problem is the determination of the shift of the Auger electron at high incident-electron energies (theory predicts that this quantity should have a constant nonzero value). The other problem is to measure the Auger line shift as a function of the angle of the emission electron. First measurements of such a dependence in the reaction (1.8) have recently been reported in a noncoincidence experiment.[115]

3. The investigation of interference between direct and resonance amplitudes and of the resonance amplitudes among themselves outside the near-threshold region. A strong dependence of the post-collision interaction effects (line shapes and positions in the spectrum) on the kinematics of the processes is expected.

4. Studies of interference between direct and resonance amplitudes in the capture of an electron by the incident ion into the continuum or into a discrete level.

During the twenty years since the first observation of PCI, there have been considerable advances in our understanding of the phenomenon. However, there are several unresolved questions.

First, there is the formation of the A–B bound state under the influence of PCI in (1.1). The problem has been partially solved for the near-threshold energy range. In this case, the capture of the slow electron (scattered electron or photoelectron) to a discrete state in the field of the ion has been observed experimentally in the form of a structure on the excitation functions of Rydberg states (see Section 3). The theoretical description of this effect has been given in terms of different models.[8,18–20,65] It is interesting to consider this effect when the electron captured into a discrete state is an autoionization electron, i.e., a fast electron, which forms a bound state with an ion or positron scattered by the atom. The interaction between all three charged particles in the final state must then be taken into account. An exact solution of this problem has been given for the case where all the particles are in the continuum and two particles have similar velocities[85] ($V_{AB} \to 0$). The solution of this problem can probably be obtained by an analytic continuation of the $V_{AB} \to 0$ case to the region $\varepsilon_{AB} < 0$. This approach was used previously[18] to solve the problem for the near-threshold region.

The other problem that is being intensively discussed in the literature, but has not as yet been fully thought out, is the transfer of angular momentum in PCI. The interaction between the scattered and autoionization electrons as they separate following the reaction can lead to the transfer of angular momentum Δl. This can affect, for example, the angular distribution of the scattered electron and its probability of capture into excited states with a particular angular momentum l. The PCI responsible for angular momentum transfer can only be the direct interaction between electrons leaving the atom.[76,107,113] Simple estimates show[53] that the momentum transfer is $\Delta l \lesssim e^2/v$, where v is the relative velocity of the electrons. In the near-threshold region, in which the velocity is large ($v > 1$), the transferred angular momentum is $\Delta l < 1$ a.u., and the angular-momentum transfer probability is low. However, this probability is greater in the

region in which the relative velocity is small ($v \ll 1$). In contrast to simple estimates, numerical calculations[63] and measurements[53] show that an angular momentum transfer $\Delta l \lesssim 2$ occurs even for low scattered-electron velocities. This can be detected experimentally by analyzing AIS excitation processes proceeding via the formation of a negative ion in the intermediate state, e.g., He($2s2p^2D$ (Refs. 76, 108, and 109). This experiment would determine the angular momentum of the slow scattered electron and would analyze the change in its angular momentum as a result of PCI. Attempts to take angular momentum into account have been undertaken[47] within the framework of the semiclassical PCI model. According to Ref. 47, it is indeed the transfer of angular momentum $\Delta l \neq 0$ that is responsible for the unexplained structure in the spectrum of Auger electrons.[56] Generally speaking, theoretical studies and experimental data on angular momentum transfer in PCI are often contradictory, and the problem requires further investigation. A further problem that has not been fully investigated in PCI theory is the influence of the scattered particle on the width Γ of the quasistationary state. All the above PCI theories assume that the scattered ion (electron) or photoelectron have no effect on the autoionization or Auger decay probability. In other words, the decay is assumed to be undistorted by the presence of a charged particle near the atom, and its interaction with decay products manifests itself only during the subsequent separation of particles in space. At the same time, although the decay occurs at a large distance from the slow scattered particle, the presence of the latter near the atom may distort the AIS wave function and modify the lifetime. The width Γ, which is regarded in all PCI theories as an adjustable parameter, may therefore differ from the AIS width of the isolated atom.[110-112] Allowance for the effect of the slow particle on the width of the quasistationary state Γ within the framework of the above PCI models should substantially improve the description of processes such as (1.1) without introducing phenomenological parameters. The resolution of these problems should result in a better understanding of the physics of the post-collision interaction.

We conclude with one important point. All the manifestations of PCI are very dependent on the parameters of the autoionizing resonances, i.e., their width, absolute magnitude, and phase of matrix elements for their excitation and decay. Effects due to the post-collision interaction can therefore be used to measure the parameters of autoionizing resonances.

It is our pleasant duty to thank M. Ya. Amus'ya for fruitful discussions of the many questions touched upon in this review.

[1]F. H. Read, Rad. Res. **64**, 23 (1975).
[2]A. Niehaus, Invited Papers and Progress Reports of X ICPEAC, North-Holland, Amsterdam, 1978, p. 185.
[3]V. I. Matveev and E. S. Parilis, Usp. Fiz. Nauk. **138**, 573 (1982) [Sov. Phys. Usp. **25**, 881 (1982)].
[4]R. B. Barker and H. W. Berry, Phys. Rev. **121**, 14 (1986).
[5]P. J. Hicks, S. Cvejanovic, J. Comer, F. H. Read, and M. J. Sharp, Vacuum **24**, 573 (1974).
[6]A. J. Smith, P. J. Hicks, F. H. Read, S. Cvejanovic, G. C. M. King, J. Comer, and J. M. Sharp, J. Phys. B **7**, L496 (1974).
[7]H. G. M. Heideman, G. Niehaus, and T. Van Ittersum, *ibid.* p. L493.
[8]G. C. King, F. H. Read, and R. C. Bradford, *ibid.* **8**, 2210 (1975).
[9]D. Spence, Phys. Rev. A **12**, 2353 (1975).
[10]H. G. M. Heideman, T. Van Ittersum, G. Nienhuis, and V. M. Hol, J. Phys. B **8**, L26 (1975).
[11]M. J. Van der Wiel, G. R. Wight, R. R. Tol, *ibid.* **9**, 15 (1976).
[12]R. Morgenstern, A. Niehaus, and U. Thielmann, Phys. Rev. Lett. **37**, 199 (1976).
[13]J. Fryar and J. W. McConkey, J. Phys. B **9**, 619 (1976).
[14]V. Schmidt, N. Sandner, W. Melhorn, and M. Y. Adam, F. Wuilleumier, Phys. Rev. Lett. **38**, 63 (1977).
[15]H. Hanashiro, Y. Suzuki, T. Sasaki, A. Mikuni, T. Takayangi, K. Wakiya, H. Suzuki, A. Danjo, T. Hino, and J. Obtanis, Phys. B **12**, L775 (1979).
[16]M. K. Bahl, R. L. Watson, and K. J. Irgollic, Phys. Rev. Lett. **42**, 165 (1979).
[17]G. Nienhuis and H. G. M. Heideman, J. Phys. B **9**, 2053 (1976).
[18]V. N. Ostrovskiĭ, Zh. Eksp. Teor. Fiz. **72**, 2079 (1977) [Sov. Phys. JETP **45**, 1092 (1977)].
[19]R. Morgenstern, A. Niehaus, and U. Thielmann, J. Phys. B **10**, 1039 (1977).
[20]A. Niehaus, *ibid.* **10**, 1845 (1977).
[21]M. Yu. Amus'ya, M. Yu. Kuchiev, S. A. Shĭenerman, W. Van de Dater, H. G. M. Heideman, Zh. Eksp. Teor. Fiz. **74**, 470 (1979) [Sov. Phys. JETP **47**, 238 (1979)].
[22]K. Helenelund, S. Hedman, L. Asplund, U. Gelius, and K. Siegbahn, Phys. Scripta **27**, 245 (1983).
[23]M. Yu. Kuchiev and S. A. Sheĭnerman, Zh. Eksp. Teor. Fiz. **90**, 1680 (1986) [Sov. Phys. JETP **63**, 986 (1986)].
[24]A. Russek and W. Mehlhorn, J. Phys. B **19**, 911 (1986).
[25]S. Ohtani, H. Nishimura, H. Suzuki, and K. Wakiya, Phys. Rev. Lett. **36**, 863 (1976).
[26]W. Hink, H. P. Schmidt, and T. Ebding, J. Phys. B **12**, L257 (1979).
[27]A. Yagishita, H. Hanashiro, S. Ohtani, and H. Suzuki, *ibid.* **14**, L777 (1981).
[28]W. Sandner and M. Volkel, *ibid.* **17**, L597 (1984).
[29]E. C. Sewell and A. Crowe, *ibid.* p. L547.
[30]D. Graf and W. Hink, Abstracts of Contributed Papers of XIL ICPEAC, Palo Alto, 1985, p. 175.
[31]R. Huster and W. Mehlhorn, Z. Phys. A **307**, 67 (1982).
[32]M. Yu. Kuchiev and S. A. Sheĭnerman, Zh. Tekh. Fiz. **57**, 1476 (1987) [Sov. Phys. Tech. Phys. **32**, 879 (1987)].
[33]W. Sandner, J. Phys. B **19**, 863 (1986).
[34]Yu. Popov, I. Bang, and J. J. Benayoun, *ibid.* **14**, 4637 (1981).
[35]A. L. Goldunov, V. N. Mileev and V. S. Senashenko, Zh. Tekh. Fiz. **53**, 436 (1983) [Sov. Phys. Tech. Phys. **28**, 273 (1983)].
[36]H. Klar, A. Franz, and H. Tenhagen, Z. Phys. D **1**, 373 (1986).
[37]P. Fano, Phys. Rev. **124**, 1866 (1961).
[38]R. Morgenstern, A. Niehaus, and U. Thielmann, J. Phys. B **9**, 363 (1976).
[39]P. Van der Straten and R.Morgenstern, *ibid.* **19**, 1361 (1986).
[40]M. Yu. Kuchiev and S. A. Sheĭnerman, Preprint PTI, Academy of Sciences, No. 963, Leningrad, 1985.
[41]G. N. Ogurtsov, J. Phys. B **16**, 745 (1983).
[42]J. Mizuno, T. Ishihara, and T. Watanabe, *ibid.* **18**, 1241 (1985).
[43]P. W. Arcuni, Phys. Rev. A **33**, 105 (1986).
[44]P. Van der Straten and P. Morgenstern, *ibid.* **34**, 4482.
[45]A. Devdeariani, V. Ostrovskii, and Yu. Sebyakin, Zh. Eksp. Teor. Fiz. **73**, 412 (1977) [Sov. Phys. JETP **46**, 215 (1977)].
[46]G. B. Armen, J. Tulkki, T. Aberg and B. Crasemann, Phys. Rev. A **36**, 5606 (1987).
[47]A. Niehaus and C. J. Zwakhals, J. Phys. B **16**, 135 (1983).
[48]J. Tulkki, G. B. Armen, T. Aberg, B. Crasemann, and M. H. Chen, Z. Phys. D **5**, 241 (1987).
[49]G. Gerber, R. Morgenstern, and A. Niehaus, J. Phys. B **6**, 493 (1973).
[50]D. G. Wilden, P. J. Hicks, and J. Comer, *ibid.* **10**, 1477 (1977).
[51]S. M. Kazakov and O. V. Khristoforov, Zh. Eksp. Teor. Fiz. **82**, 1772 (1982) [Sov. Phys. JETP **55**, 1023 (1982)].
[52]D. Spence, J. Phys. B **11**, 243 (1978).
[53]Van Ittersham, H. G. M. Heideman, G. Niehaus, and J. Prins, *ibid.* **9**, 1713 (1976).
[54]T. C. Chiang, D. E. Easman, F. J. Himpel, G. Kaindl, and M. Aono, Phys. Rev. Lett. **45**, 1846 (1980).
[55]V. Schmidt, S. Krummacher, F. Wuilleumier, and P. Dhez, Phys. Rev. A **24**, 1803 (1981).
[56]S. Hedman, K. Helenelund, L. Asplund, U. Gelius, and K. Siegbahn, J. Phys. B **15**, 799 (1982).
[57]S. Southworth, U. Becker, C. M. Truesdale, P. H. Kobrin, D. W. Lindle, S. Owaki, and D. A. Shirley, Phys. Rev. A **28**, 261 (1983).
[58]G. B. Armen, T. Aberg, J. C. Levin, B. Craseman, M. H. Chen, G. E. Ice, and G. S. Brown, Phys. Rev. Lett. **54**, 1142 (1985).
[59]M. Borst and V. Schmidt, Phys. Rev. A **33**, 4456 (1986).
[60]G. Nienhuis and H. G. M. Heideman, J. Phys. B **8**, 2225 (1975).

[61]D. J. Thouless, *Quantum Mechanics of Many-Body Systems*, Academic Press, NY, 1973 [Russ. transl. Mir, M., 1975].
[62]M. Ya. Amus'ya, N. H. Cherepkov, and L. V. Chernysheva, Zh. Eksp. Teor. Fiz. **60**, 160 (1971) [Sov. Phys. JETP **33**, 90 (1971)].
[63]M. Ya. Amusia, M. Yu. Kuchiev, and S. A. Sheĭnerman, *Coherence and Correlation in Atomic Collisions*, Plenum, NY, 1980, p. 297.
[64]S. A. Sheĭnerman, M. Ya. Amus'ya, and M. Yu. Kuchiev, Preprint from the Ioffe Physicotechnical Institute, No. 777, Leningrad, 1982.
[65]M. Ya. Amusia, M. Yu. Kuchiev, S. A. Sheĭnerman, and S. I. Sheftel, J. Phys. B **10**, 535 (1977).
[66]J. Mizuno, T. Ishihara, and T. Watanabe, J. Phys. B **17**, 85 (1984).
[67]M. Yu. Kuchiev and S. A. Sheĭnerman, *ibid.* **18**, 551 (1985).
[68]M. Yu. Kuchiev and S. A. Sheĭnerman, Comp. Phys. Comm. **39**, 155 (1986).
[69]S. A. Sheĭnerman and M. Yu. Kuchiev, Preprint from the Ioffe Physicotechnical Institute, No. 977, Leningrad, 1985.
[70]M. Yu. Kuchiev and S. A. Sheĭnerman, Izv. Akad. Nauk SSSR. Ser. Fiz. **50**, 1390 (1986) [Bull. Acad. Sci. USSR Phys. Ser. **50** (7), 144 (1986)].
[71]F. H. Read, J. Phys. B **10**, 207 (1977).
[72]G. Gerber and A. Niehaus, *ibid.* **9**, 123 (1976).
[73]Q. C. Kessel, R. Morgenstern, B. Muller, A. Niehaus and U. Thielmann, Phys. Rev. Lett. **40**,645 (1978).
[74]J. A. Baxter, J. Comer, P. J. Hicks, and W. J. McConkey, J. Phys. B **12**, 2031 (1979).
[75]C. Bottcher and K. R. Schneider, *ibid.* **8**, 911 (1976).
[76]W. Van de Water, H. G. M. Heideman, and G. Nienhuis, *ibid.* **14**, 2935 (1981).
[77]K. Helenelund, S. Hedman, L. Asplund, U. Gelius, K. Siegbahn, P. Froelich, and O. Goscinski, Int. Conf. on X-Ray and Inner-shell Processes, Abstracts, Leipzig **1**, 184 (1984).
[78]P. Froelich, O. Goscinski, U. Gelius, and K. Helenelund, J. Phys. B **17**, 979 (1984).
[79]K. Helenelund, U. Gelius, P. Froelich, and O. Goscinski, *ibid.* **19**, 379 (1986).
[80]P. Froelich, O. Goscinski, U. Gelius, and K. Helenelund, *ibid.* **19**, 379 (1986).
[81]F. H. Read, private communication, 1987.
[82]M. Yu. Kuchiev and S. A. Sheĭnerman, Proceedings of the Third Scientific Seminar on Autoionization Phenomena in Atoms [in Russian], Moscow University Press, Moscow, 1987, p. 38.
[83]P. W. Arcuni and D. Schneider, Phys. Rev. A **36**, 3059 (1987).
[84]G. B. Armen, S. L. Sorensen, S. W. Whitfield, G. E. Ice, J. C. Levion, G. S. Brown, and B. Crasemann, *ibid.* **35**, 3966.
[85]M. Yu. Kuchiev and S. A. Sheĭnerman, J. Phys. B **21**, 2027 (1988).
[86]M. Branner and J. S. Briggs, *ibid.* **19**, 325 (1986).
[87]T. Watanabe, T. Ishihara, and J. Mizuno, *ibid.* **16**, 107 (1983).
[88]J. Mizuno, T. Ishihara, and T. Watanabe, Abstracts of Contributed Papers presented at XII ICPEAC, Gattlinburg, 1981, p. 253.
[89]G. H. Wannier, Phys. Rev. **90**, 817 (1953).
[90]G. Stefani, L. Alvalid, A. Lahman-Bennani, and A. Duguet, see Ref. 30, p. 176.
[91]G. Stefani, L. Alvalid, A. Lahman-Bennani, and A. Duguet, J. Phys. **B19**, 3787 (1986).
[92]K. Wakiya, H. Suzuki, T. Takayanagi, M. Muto, S. Ito, Y. Iketaki, and S. Ohtani, see Ref. 88, p. 247.
[93]W. Mehlhorn, Atomic Physics 8: Proc. of the 8th ICAP, Plenum, London, 1983, p. 213.
[94]K. Siegbahn, *ibid.* 243.
[95]D. Graf and W. Hink, J. Phys. B **18**, 803 (1985).
[96]D. Graf and W. Hink, *ibid.* **19**, 221 (1986).
[97]R. Huster, W. Sandner, and W. Mehlhorn, *ibid.* **20**, 287 (1987).
[98]G. N. Ogurtsov, V. M. Mikoushkin, and I. P. Flaks, European Conference on Atomic Physics, Book of Abstracts, Heidelberg **11**, 759 (1981).
[99]A. Yagishita, H. Suzuki, S. Ohtani, and H. Hanashiro, see Ref. 88, p. 249.
[100]R. A. Peterokop, *Theory of Ionization of Atoms by Electron Impact* [in Russian], Zinatne, Riga, 1975.
[101]A. Burgess and I. C. Percival, Adv. At. and Mol. Phys. **4**, 109 (1968).
[102]M. Volkel, M. Schnetz, and W. Sandner, Abstracts of Contributed Papers of XV ICPEAC, Brighton, U.K., 1987, p. 258.
[103]M. Inokuti, Rev. Mod. Phys. **43**, 297 (1971).
[104]D. Graf, K. Starke, and W. Hink, see Ref. 102, p. 257.
[105]A. Bordenave-Montesquive, A. Gleizes and P. Benoit-Cattin, Phys. Rev. A **25**, 245 (1982).
[106]M. Yu Kuchiev and S. A. Sheĭnerman, Pis'ma Zh. Tekh. Fiz. **13**, 1001 (1987) [Sov. Tech. Phys. Lett. **13**, 417 (1987)].
[107]W. Van de Dater and H. G. M. Heideman, see Ref. 88, p. 243.
[108]W. Van de Dater and H. G. M. Heideman, J. Phys. B **14**, 1065 (1981).
[109]P. J. M. Van der Burgt and H. G. M. Heideman, *ibid.* **20**, 4605 (1987).
[110]N. Stolterfoht, D. Brandt, and M. Prost, Phys. Rev. Lett. **43**, 1654 (1979).
[111]V. I. Matveev and E. S. Parilis, Pis'ma Zh. Tekh. Fiz. **5**, 297 (1979) [Sov. Tech. Phys. Lett. **5**, 120 (1979)].
[112]V. I. Matveev and E. S. Parilis, Zh. Tekh. Fiz. **51**, 1792 (1981) [Sov. Phys. Tech. Phys. **26**, 1039 (1981)].
[113]P. J. M. Van der Burgt, J. Van Eck, H. G. M. Heideman, and G. Niehaus, see Ref. 30, p. 156.
[114]D. Sh. Kunikeev and V. S. Senashenko, see Ref. 102, Late Contributed Papers, p. 17.
[115]V. N. Mikushkin, Abstracts of papers presented at the Tenth Conf. on Electron. At. Coll. [in Russian], Uzhgorod **1**, 17 (1988).
[116]L. P. Gor'kov and L. P. Pitaevskiĭ, Dokl. Akad. Nauk SSSR **151**, 822 (1963) [Sov. Phys. Dokl. **8**, 788 (1964)].
[117]C. Herring and M. Flicker, Phys. Rev. A **134**, 362 (1964).
[118]V. N. Galitskiĭ, E. E. Nikitin, and B. N. Smirnov, *Theory of Atomic Collisions* [in Russian], Nauka, M., 1981.
[119]M. Yu. Kuchiev, J. Phys. B **18**, 579 (1985).

Translated by S. Chomet